BINARY PROPERTIES FROM CEPHEID RADIAL VELOCITIES (CRaV)

The Astronomical Journal, 150:13 (18pp), 2015 July doi:10.1088/0004-6256/150/1/13

BINARY PROPERTIES FROM CEPHEID RADIAL VELOCITIES (CRaV)

Nancy Remage Evans[1], Leonid Berdnikov[2,3], Jennifer Lauer[4], Douglas Morgan[4], Joy Nichols[4], H. Moritz Günther[5,6], Natalya Gorynya[7,8], Alexey Rastorguev[8], and Pawel Moskalik[9]
[1] Smithsonian Astrophysical Observatory, MS 4, 60 Garden St., Cambridge, MA 02138, USA; nevans@cfa.harvard.edu
[2] Astronomy and Astrophysics Research Division, Entoto Observatory and Research Center, P.O. Box 8412, Addis Ababa, Ethiopia
[3] Sternberg Astronomical Institute of the Moscow State University, 13 Universitetskii Prospect, Moscow 119992, Russia and Isaac Newton Institute of Chile, Moscow Branch, 13 Universitetskij Prospect Moscow 119992, Russia
[4] Smithsonian Astrophysical Observatory, MS 34, 60 Garden St., Cambridge, MA 02138, USA
[5] Smithsonian Astrophysical Observatory, MS 6, 60 Garden St., Cambridge, MA 02138, USA
[6] Massachusetts Institute of Technology, Kavli Institute for Astrophysics and Space Research, 77 Massachusetts Avenue, Cambridge, MA 02139, USA
[7] Institute of Astronomy, Russian Academy of Sciences, 48 Pyatnitskaya Str., Moscow, Russia
[8] Lomonosov Moscow State University, Sternberg State Astronomical Institute, 13 Universitetskii Prosp., Moscow, Russia
[9] Copernicus Astronomical Center, Warsaw, Poland
Received 2014 December 11; accepted 2015 May 5; published 2015 June 19

ABSTRACT

We have examined high accuracy radial velocities of Cepheids to determine the binary frequency. The data are largely from the CORAVEL spectrophotometer and the Moscow version, with a typical uncertainty of $\leqslant 1$ km s^{-1}, and a time span from 1 to 20 years. A systemic velocity was obtained by removing the pulsation component using a high order Fourier series. From this data we have developed a list of stars showing no orbital velocity larger than ± 1 km s^{-1}. The binary fraction was analyzed as a function of magnitude, and yields an apparent decrease in this fraction for fainter stars. We interpret this as incompleteness at fainter magnitudes, and derive the preferred binary fraction of $29\% \pm 8\%$ ($20\% \pm 6\%$ per decade of orbital period) from the brightest 40 stars. A comparison of this fraction in this period range (1–20 years) implies a large fraction for the full period range. This is reasonable in that the high accuracy velocities are sensitive to the longer periods and smaller orbital velocity amplitudes in the period range sampled here. Thus the Cepheid velocity sample provides a sensitive detection in the period range between short period spectroscopic binaries and resolved companions. The recent identification of δ Cep as a binary with very low amplitude and high eccentricity underscores the fact that the binary fractions we derive are lower limits, to which other low amplitude systems will probably be added. The mass ratio (q) distribution derived from ultraviolet observations of the secondary is consistent with a flat distribution for the applicable period range (1–20 years).

Key words: binaries: general – stars: massive – stars: variables: Cepheids – techniques: radial velocities

Supporting material: tar.gz file, machine-readable and VO tables

1. INTRODUCTION

Star formation is a very active area of research both observationally and theoretically, with many unanswered questions. One such area is binary and multiple systems. They are very common and their formation involves both disk fragmentation and accretion. Binaries are particularly important for a number of reasons. They result in redistribution of angular momentum during formation and have an important effect on the distribution of masses, the Initial Mass Function. Furthermore, stars on the zero-age main sequence (ZAMS) are at their minimum radius, and hence as they evolve and expand, some binary stars will diverge in their evolution from single stars if they become large enough to undergo Roche lobe overflow. For the most massive stars (O stars) it has recently been estimated that more than 70% will exchange mass through this process (Sana et al. 2012), and a third of those will merge. This has a dramatic effect on the predictions for post-main sequence evolution. It is important to determine what fraction of less massive B stars meets this fate. Furthermore, high mass stars are destined to become compact objects. Some of those in binary systems will ultimately provide a zoo of exotic end-stage objects: symbiotic stars, novae, cataclysmic variable stars, supernovae. For all these reasons, we need to determine the properties of the population of binaries in order to link these stages together. (In this paper we will use "binaries" as short hand for binaries or higher order multiple systems. Indeed, in many contexts the tightest subsystem in a multiple functions as a binary.)

In order to untangle and understand all these processes, binary properties are needed as a function of stellar mass, binary mass ratio, and separation. Because star formation covers many decades of separation (with very different properties of the "raw material") from the beginning of the collapse to the ZAMS, it is probable that binary properties also differ depending on, for instance, the separation. We begin by summarizing what is known about binary properties of stars with different masses.

Solar mass stars: Binary properties of low mass stars are reasonably well known, notably through the seminal study of Duquennoy & Mayor (1991). The combination of CORAVEL velocities (below) with visual binary results and common proper motion pairs produced a distribution of binary periods which has become the cornerstone of the discussion of binary systems. The recent study of Raghavan et al. (2010) expanded the results considerably, and Tokovinin (2014) added further discussion of hierarchical multiples.

O stars: Properties of massive and intermediate mass stars (O and B) stars are less well determined. They are rarer, and hence typically more distant. Their spectral lines are broad, and hence velocities cannot be as precisely determined as for cooler

stars. Finally, particularly for the most massive stars (O stars) the interpretation is complicated by high rotation and continuous mass loss. O star binary properties have been discussed by Sana et al. (2013) and Kimiki & Kobulnicky (2012) and references therein, as well as Kobulnicky et al. (2014), Caballero-Nieves et al. (2014) and Aldoretta et al. (2015).

B stars: B stars provide a valuable step in tracing the progression of binary properties from low mass to high mass, and largely avoid the complications of mass loss in interpretation. Radial velocity studies of B stars date back many years. Wolff (1978) found that approximately 24% of late B stars are binaries with periods <100 days and mass ratios $M_2/M_1 > 0.1$. Abt, and coworkers (e.g., Abt et al. 1990) combined radial velocities with visual binaries and common proper motion stars for B stars and discussed the implications for star formation. Similar work was done by Levato et al. (1987).

Binary studies of B stars have been enhanced greatly by interferometry and high resolution imaging techniques. For instance, using speckle interferometry, Mason et al. (2009) found that 64% of the B stars in their OB star sample had companions with $\Delta V < 3$ mag between $0\farcs03$ and $5''$ separation. However, many stars were included on the target list because they already showed some indication of being binary (B.D. Mason 2014, private communication), so the sample is not unbiased. Intermediate mass stars binaries in Sco OB2 were studied by Kouwenhoven et al. (2007), who found a binary fraction of >70%. Shatsky & Tokovinin (2002) made an adaptive optics survey of the B stars in Sco OB2, identifying essentially all companions with separations between 45 and 900 AU. They found a companion star fraction of 0.20 ± 0.04 per decade of separation.

A stars: Binary properties of A stars (only slightly less massive than B stars) are discussed by De Rosa et al. (2014). They find a different distribution of mass ratios for separations smaller and larger than 125 AU (a period of 570 years). They find 44% of their volume limited sample is binary or multiple.

Stellar multiplicity over all masses and separations was recently summarized by Duchene & Krauss (2013), who find an increasing multiplicity fraction with increasing mass.

Cepheids: Studies to identify and characterize binary Cepheids have been numerous, particularly in the effort to measure masses to provide information to resolve "the Cepheid mass problem." Cepheids, which began on the main sequence as B stars, provide several ways to improve our knowledge of binary properties of intermediate mass stars. It is the aim of the present study to use Cepheid velocities to contribute to our understanding of binary properties of intermediate and massive stars. A variety of techniques have been used to determine the distributions of periods and mass ratios of Cepheids. Two recent summaries are provided by Szabados[10] and by Evans et al. (2013).

We have undertaken three related studies to determine the properties of intermediate mass stars, in particular Cepheids, and their progenitor B stars. This is both to determine whether the consequences of binarity are as severe as for O stars, and also because some binary properties can be particularly well determined making use of the characteristics of these stars. In this study we focus on a property of Cepheids which sets them apart from their main sequence counterparts, namely their sharp spectral lines and accurate velocities. This classic approach to binary studies lets us probe both systems with periods longer than a few days and also systems with low mass secondaries. In the second approach, we use X-ray studies of late B stars to determine the fraction which have low mass companions (Evans et al. 2011). Late B stars themselves do not in general produce X-rays, but companions later than mid-F spectral type are copious X-ray producers at the young age of the system. Thus low mass companions can be identified through X-ray observations of late B stars in a cluster. Third, we have made a survey with the *Hubble Space Telescope* (*HST*) Wide Field Camera 3 to determine the properties of resolved companions of Cepheids (Evans et al. 2013). This study demonstrates another contribution Cepheids can make to the understanding of binaries. Since many companions dominate in the satellite ultraviolet, the mass of the secondary, and hence the mass ratio, can be determined from an uncontaminated spectrum.

Ultimately, this combination of techniques will enable us to provide a much improved description of the binary properties of these intermediate mass stars. There is one feature of Cepheids, however, which makes their binary properties more difficult to interpret (or possibly will help us get a handle on another aspect of binarity). Since Cepheids are post red-giant branch stars, short period binary systems have undergone interactions, presumably resulting in mergers in a number of cases. Indeed, the shortest period system in the Milky Way containing a Cepheid has an orbital period of a year (Sugars & Evans 1996). An additional complication to the interpretation is that multiple systems may undergo dynamical evolution until they reach a stable hierarchical state. A component (typically the smallest) may be ejected from the system in the process.

The advent of correlation spectrometers vastly increased the quantity of accurate radial velocities available for Cepheids. The CORAVEL instrument at the Geneva observatory (Baranne et al. 1979) observed a large number of Cepheids for studies of galactic structure and to obtain Cepheid distances via a variant of the Baade Wesselink technique. The accuracy of the velocities is typically less than 1 km s^{-1} in the magnitude range of the stars in this study. A similar instrument was built at Moscow University (Tokovinin 1987). Between these instruments (including an extension to the southern hemisphere), a large number of Cepheids has been observed since 1978. A major purpose of these observations was to discover binaries which can then be used to measure Cepheid masses.

1.1. The Scope of This Project

While radial velocity spectrometers have produced a huge amount of velocity data for Cepheids, the data have never been analyzed to determine the fraction of stars which show no orbital motion over the more than three decades they cover. That is the goal of this project, Cepheid Radial Velocities (CRaV). Many Cepheids have been identified as binary systems. However, the binary frequency is only obtained if we know how many single stars are also included in the sample. The main aim of this project is to examine the sample of stars for orbital motion, or in its absence, to produce a well characterized sample of stars without orbital motion. We have deliberately limited the data examined to observations with a typical accuracy of 1 km s^{-1} per observation and studies which included many Cepheids to allow cross-checks on the accuracy. In this first paper, we include data from 1978 to 2000 of "northern stars" down to $-20\fdg9$ (as discussed below). We plan

[10] http://www.konkoly.hu/CEP/orbit.html

two subsequent papers on southern stars and observations since 2000. As discussed in the detection limits section, with this sample, we will detect almost all binaries with orbital periods of 1–20 years down to mass ratios $q = M_2/M_1 = 0.1$ (where M_1 is $\geqslant M_2$), that is companions as cool as K stars.

We begin with the 38 stars in Table 2 which meet these criteria, omitting stars known to be binary. To complete the analysis, we examine all stars brighter than 9th magnitude (Table 6, 62 stars), ultimately omitting stars deemed to have too little information.

The purpose of CRaV is to investigate the annual mean systemic velocities of Cepheids with accurate velocities. The observed Cepheid velocity, of course, is a combination of the systemic velocity of the star and the pulsation velocity curve. To correct for the pulsation velocity, we use a Fourier representation of the curve with up to 20 terms. The velocity curves have to be aligned over decades by means of a pulsation period. Both these steps will be discussed in sections below. Finally, cross-checking the results of the annual means between studies identifies and removes small systematic differences.

2. THE SAMPLE

The accuracy with which a Cepheid velocity can be measured ($1\,\mathrm{km\,s^{-1}}$) is easily the highest for high and intermediate mass stars. While this accuracy in the annual means does not come close to the highest accuracy possible today (e.g., Anderson 2014), the long sequence of data at this level is valuable. The details of the sample which is available at this level of accuracy are discussed in this section.

The Moscow velocities (Gorynya et al. 1992, 1996, 1998, referred to as Gorynya et al. below) are a large dataset for which many stars are covered annually in the 1990s. For this reason, we are defining our "northern sample" to be stars with decl. $> -20\overset{\circ}{.}9$, the region they covered.

For the most southern stars in the sample, data from a few studies have been deferred to the next paper (southern stars) so that we can assess the zeropoints of the whole study. Datasets in this category are Petterson et al. (2004), Coulson & Caldwell (1985), Coulson et al. (1985), Gieren (1981) and Caldwell et al. (2001). On the other hand, CORAVEL data from both Observatoire de Haute-Provence and ESO La Silla (Bersier et al. 1994 and Bersier 2002) have been included since they were taken and analyzed with the N hemisphere stars by the Geneva group.

The sample consists of Cepheids brighter than 9.0 mag north of decl. $-20\overset{\circ}{.}9$, not already known to be binaries. There are a few stars which otherwise fall within these criteria which we have not included. We have not used double mode pulsators (CO Aur, TU Cas, and EW Sct) because of the complexity of their light and velocity curves. We have also omitted V473 Lyr, the only Cepheid know to have Blazhko-like variations in amplitude. RY CMa did not have a well covered velocity curve during a single season, making a Fourier fit unreliable.

Table 1 lists the sources of data used in the study and Table 2 summarizes the data used for each of the stars. Period and $\langle V \rangle$ are taken from Fernie et al. (1995) (except for CK Cam, which is from Berdnikov et al. 2000). The farthest right column identifies stars pulsating in an overtone mode, based on the discussion of Evans et al. (2015). IR Cep is also classified as an overtone (Groenewegen & Oudmaijer 2000).

During the course of this project, relevant data, means, and other parameters such as Fourier coefficients were stored in a database (created by D. Morgan). This proved invaluable for tracking the steps, and occasional updating as needed.

Table 1
Sources

Id	Symbol Table	Symbol Plot[a]	Source
1	gg	r circle	Gorynya et al. (1992, 1996, 1998)
2	b9	r diamond	Bersier et al. (1994)
3	im	c^	Imbert (1999)
4	ba	g x	Barnes et al. (2005)
5	kk	m x	Kiss & Vinko (2000)
6	b0	y diamond	Bersier (2002)
7	s4	c square	Storm et al. (2004)

Note.
[a] r—red; c—cyan; g—green; y—yellow; m—magenta.

3. DATA TREATMENT

3.1. Fourier Curves

In order to remove the pulsation velocity from the observed velocity, we (LB) fit the pulsation curve with a Fourier series. In general, all the data from Gorynya et al. sources were fit in order to get well determined curves tightly constrained by the data. Occasionally other data were included to obtain a well covered pulsation cycle. (Exceptions were also sometimes made for stars with more difficult periods as discussed in the next section.) With this data up to 20 Fourier coefficients are needed from the fit. Note that one reason for restricting the sample to stars with velocity curves which are well covered by high accuracy data is that this quality and quantity of data is required for a Fourier fit which will provide a pulsation velocity for any phase with the necessary accuracy ($1\,\mathrm{km\,s^{-1}}$).

The pulsation curve is well represented by a Fourier series:

$$V_R = c(0) + \sum_{i=1}^{10} \left(a_i \sin(2\pi i \phi) + b_i \cos(2\pi i \phi) \right)$$

where V_R is the radial velocity, $c(0)$ is the systemic velocity, ϕ is the phase, a_i and b_i are the Fourier coefficients, and i runs from 1 to 10 (as needed).

A sample curve is provided in Figure 1 showing the data for FN Aql from Gorynya et al. for 1989, and the Fourier representation. The Fourier coefficients for each star are listed at http://hea-www.cfa.harvard.edu/~evans/.

The fitting process also determined a period and epoch of maximum light which is included in the table on the website. While this period should be used to generate the Fourier plot, it should *not* be used when data taken over many years are to be phased together. As needed, the phase shift between the two periods was incorporated in the analysis. (Fourier coefficients for S Vul and SV Vul are included, although ultimately the means used were from independent year by year solutions as discussed in the Appendix.)

3.2. Pulsation Periods

Cepheids have famously repetitive light variations. For most stars we have been able to identify a constant period or variation in period which has been parametrized as a parabola (changing period). Using these well determined periods, largely derived from photometry, phases were computed for

Table 2
Data Sources

Star	1[a]	2[a]	3[a]	4[a]	5[a]	6[a]	7[a]	P (d)	$\langle V \rangle$ (mag)	Mode
ηAql	gg	⋯	⋯	ba	kk	b0	s4	7.17	3.90	⋯
SZ Aql	⋯	⋯	⋯	ba	⋯	b0	⋯	17.14	8.60	⋯
TT Aql	gg	b9	im	ba	⋯	b0	⋯	13.75	7.14	⋯
FM Aql	gg	⋯	⋯	ba	⋯	⋯	⋯	6.11	8.27	⋯
FN Aql	gg	⋯	⋯	ba	⋯	⋯	⋯	9.48	8.38	⋯
V1162 Aql	gg	⋯	⋯	⋯	⋯	⋯	⋯	5.38	7.80	⋯
RT Aur	gg	⋯	⋯	⋯	kk	⋯	⋯	3.73	5.45	⋯
RX Aur	gg	⋯	im	⋯	⋯	⋯	⋯	11.62	7.66	⋯
CK Cam	gg	⋯	⋯	⋯	kk	⋯	⋯	3.29	7.54	⋯
SU Cas	gg	b9	⋯	⋯	kk	⋯	s4	2.74	5.99	o
V379 Cas	gg	⋯	⋯	⋯	⋯	⋯	⋯	4.31	9.05	o
V636 Cas	gg	b9	⋯	⋯	⋯	⋯	⋯	8.38	7.20	⋯
δ Cep	⋯	b9	⋯	ba	kk	⋯	s4	5.37	3.99	⋯
IR Cep	gg	⋯	⋯	⋯	⋯	⋯	⋯	2.98	7.78	o
X Cyg	gg	b9	⋯	ba	kk	⋯	s4	16.39	6.39	⋯
CD Cyg	gg	⋯	im	⋯	⋯	⋯	⋯	17.07	8.95	⋯
DT Cyg	gg	b9	⋯	⋯	kk	⋯	⋯	3.53	5.77	o
V1726 Cyg	gg	⋯	⋯	⋯	⋯	⋯	⋯	4.24	9.01	o
ζ Gem	gg	b9	⋯	⋯	kk	⋯	⋯	10.15	3.92	⋯
W Gem	gg	⋯	im	⋯	⋯	⋯	⋯	7.91	6.95	⋯
V Lac	gg	⋯	⋯	⋯	⋯	⋯	⋯	4.98	8.94	⋯
X Lac	gg	b9	⋯	ba	⋯	⋯	⋯	5.44	8.41	o?
RR Lac	gg	b9	im	⋯	⋯	⋯	⋯	6.42	8.85	⋯
BG Lac	⋯	⋯	im	ba	⋯	⋯	⋯	5.33	8.88	⋯
SV Mon	gg	⋯	im	⋯	⋯	⋯	⋯	15.23	8.22	⋯
Y Oph	gg	⋯	⋯	⋯	⋯	⋯	⋯	17.13	6.17	⋯
RS Ori	gg	⋯	im	⋯	⋯	⋯	⋯	7.57	8.41	⋯
V440 Per	gg	b9	⋯	⋯	⋯	⋯	⋯	10.94	6.28	o
U Sgr	gg	b9	⋯	⋯	⋯	b0	s4	6.75	6.70	⋯
WZ Sgr	gg	⋯	⋯	⋯	⋯	b0	⋯	21.85	8.03	⋯
BB Sgr	gg	⋯	⋯	⋯	⋯	⋯	⋯	6.64	6.95	⋯
ST Tau	gg	b9	im	⋯	⋯	⋯	⋯	4.03	8.22	⋯
SZ Tau	gg	b9	⋯	⋯	kk	⋯	⋯	4.47	6.53	o
EU Tau	gg	b9	⋯	⋯	⋯	⋯	⋯	2.97	8.09	o
S Vul	gg	⋯	⋯	⋯	⋯	⋯	⋯	68.46	8.96	⋯
T Vul	⋯	b9	⋯	ba	kk	⋯	⋯	4.43	5.76	⋯
X Vul	gg	b9	⋯	⋯	⋯	⋯	⋯	6.32	8.85	⋯
SV Vul	gg	b9	im	ba	kk	⋯	s4	44.99	7.22	⋯
	⋯	⋯	⋯	⋯	⋯	⋯	⋯	⋯	⋯	

Note.
[a] Data sources identified in Table 1.

the velocity measures. Combining these velocities with the Fourier representation resulted in the mean velocity difference for the observations for each year, as discussed in the next section. With this approach assuming the phase from the periods in the Fourier fit (http://hea-www.cfa.harvard.edu/~evans/), years in which comparatively few observations were obtained still provide a mean velocity.

In a few cases pulsation periods are too unstable for long term projection. Long period–high luminosity stars sometimes fall in this category (S Vul, and SV Vul). Stars pulsating in an overtone also seem to have unusually large period variations (Szabados 1983; Berdnikov et al. 1997; Evans et al. 2015). Some stars in these groups have period fluctuations on longer timescales than the 20 years discussed here, so a single period was adequate to phase the data. Since it is desirable to have binary information on both high mass (long period stars) and overtone pulsators, in some cases we have adopted a more complicated approach. Specifically, for four stars (EU Tau, SV Mon, ST Tau, and X Lac) we had to develop an individual approach to the phasing of the curves, typically based on photometric curves. Details are provided in the Appendix. Working through the sample, we became aware that the 5^{d} Cepheid X Lac has an unusually erratic period. Because of this we suggest that it may be pulsating in the first overtone. Various diagnostics of overtone pulsation are considered in the case of X Lac and discussed in the Appendix.

Where the periods are erratic (SV Vul, and S Vul) fits to the velocity curve for each year have been made. The fits produce the amplitude of the curve, the phase of maximum light, and also the mean velocity without assuming a predicted period. For these cases we are restricted to seasons with a significant amount of data to obtain the systemic (γ) velocity corrected for pulsation. We do not include these seasonal means in the final cross check on annual means of individual data sets (see Section 5). All these stars for which we have used a special approach are discussed in the Appendix.

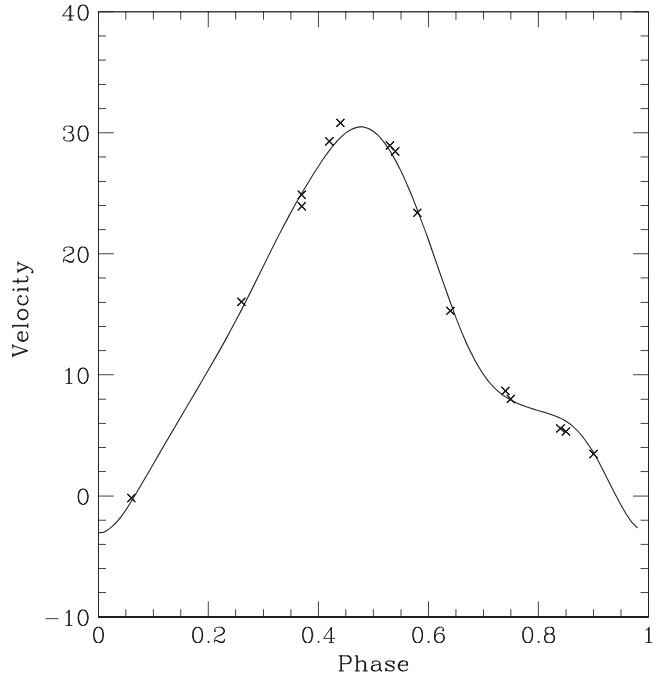

Figure 1. Sample velocity curve for FN Aql. Solid line is the Fourier fit; the data (shown with x) are from Gorynya et al. for the year 1989. Velocities are in km s^{-1}. As is typical, the Fourier fit was made using the Gorynya et al. data for all seasons (79 points in total).

3.3. Cepheid Velocities

This section discusses the way in which the Fourier curves, velocity data, and periods are used to generate annual mean systemic (γ) velocities for the Cepheids.

When the period varied a little (or was a little different from the one in the Fourier fits), we made an adjustment with small phase shifts. This may sound arbitrary, but in cases of stars with erratic variations or even a constantly changing period, the single best group of data (typically the Gorynya et al. velocities) was required to tightly constrain the Fourier fit. Only high quality data providing a well covered pulsation cycle will constrain the Fourier fit to the level of accuracy needed in the project (<1 km s^{-1}). To emphasize, the period in the Fourier coefficient table is the one that should be used to generate the Fourier curve. Any deviation from that period during the whole time span of the data was included with a subsequent phase shift. The next step is to compare data from each season with the Fourier curve. The average difference between the data and the curve is computed, creating the annual mean velocity. As discussed in the next section, a small instrumental correction was computed for each instrument for each season using all Cepheids (Table 3). The annual mean velocity from the data and the Fourier curves is listed in Table 4. Columns in Table 4 list the star, the data source, the year, the mean and standard deviation σ and the number of observations. The corrections in Table 3 have been included.

Since Cepheids occur close to the galactic plane instead of randomly over the sky, observations are typically confined to a season. Hence, the division of velocities by calender year is appropriate. For Cepheids in the winter sky, some observations from a given source might be taken in December, with related observations in the following January. We have investigated whether division of these stars by calendar year affects our results. For Cepheid periods the optimal cadence is typically at least a day. Many of the observations were taken during observing runs of a month, often with more than one run a year. We have examined the few instances where a star had a December–January combination of observations and found that only a very few points would be assigned to a different year in a more complicated scheme, so adding complexity does not seem warranted in deriving the annual mean velocities.

Table 3
Annual Corrections

Source	Year	Mean (km s^{-1})	σ (km s^{-1})	N
gg	1986	0.16	0.19	1
gg	1987	0.71[a]	0.17	6
gg	1989	0.25	0.07	3
gg	1990	0.41[a]	0.10	6
gg	1991	0.35[a]	0.04	20
gg	1992	0.25	0.07	10
gg	1993	−0.39[a]	0.09	16
gg	1994	−0.34[a]	0.05	22
gg	1995	−0.42[a]	0.04	23
gg	1996	0.08	0.04	22
gg	1997	0.17	0.06	17
gg	1998	0.18	0.10	12
b0	1978	−0.16	0.06	4
b0	1979	−0.38[a]	0.07	4
b0	1980	0.30	0.08	4
b0	1981	0.02	0.12	4
b0	1982	−0.69	0.39	1
b0	1987	−0.22	0.17	3
b0	1988	−0.85	0.37	3

Note.
[a] Corrections incorporated in Table 4.

(This table is available in machine-readable and Virtual Observatory (VO) forms.)

Table 4
Cepheid Annual Mean Velocities

Star	Source	Year	Mean (km s^{-1})	σ (km s^{-1})	N
Eta Aql	b0	1983	0.74	0.48	5
Eta Aql	gg	1986	0.16	0.19	25
Eta Aql	s4	1986	0.12	0.28	25
Eta Aql	b0	1989	0.37	0.36	33
Eta Aql	ba	1995	2.71	⋯	1
Eta Aql	kk	1996	0.58	0.33	8
Eta Aql	ba	1996	1.14	0.51	13
Eta Aql	ba	1997	−0.05	0.51	16
Eta Aql	kk	1997	0.71	0.30	6
SZ Aql	b0	1996	−0.38	0.24	21
SZ Aql	ba	1996	−0.16	0.23	13
SZ Aql	ba	1997	−0.15	0.27	19
SZ Aql	b0	1997	−0.29	0.57	10
TT Aql	im	1989	−0.07	0.18	14
TT Aql	im	1991	0.28	0.12	5
TT Aql	im	1993	−0.14	0.45	5

(This table is available in its entirety in machine-readable and Virtual Observatory (VO) forms.)

3.4. Annual Corrections

In this project we examine the annual means of the velocity data for each star (corrected for pulsation velocity) to identify any long term variation due to orbital motion. Even though the datasets we have used were taken with high dispersion and well controlled instruments, in order to make comparisons to the desired accuracy over two decades, we have made the following check. To test for small instrumental zero point variations, we have formed the mean and standard deviation (σ) of all stars observed in each season for each instrument. From this we have created small annual corrections to be incorporated in the analysis, listed in Table 3. Columns in Table 3 are the data source (Table 2), the year, mean and standard deviation, and the number of stars. Corrections $>0.3\,\mathrm{km\,s^{-1}}$ (absolute value) from at least 4 stars (indicated with a) have been added to Table 4 and Figure 2. Using corrections derived from a smaller number of stars puts too large a weight on individual stars, i.e., corrects a possible orbital variation to 0.0. In Table 3, Column 5, an entry for only 1 star lists s.d. of the fit of that data to the Fourier curve as the error. A sense of the overall velocity comparison between instruments can also be obtained from Table 3.

4. RESULTS

The results from this study are presented in Figure 2, showing the annual mean systemic (γ) velocity as a function of year. Included in the plots is the band of $\pm 1\,\mathrm{km\,s^{-1}}$. The symbols for each data source are listed in Table 1. Seasons with only one observation have been omitted from the plots.

4.1. Window Function

Our data sample is drawn from the literature using data which was not designed for evenly spaced long term coverage to identify binaries. We have performed the following check to see how thoroughly the dataset covers the frequency (period) space. This test was suggested by the discussion of the optimal observing sequence developed for the *HST* Cepheid Key Project (Freedman et al. 1994). We examined the window functions produced by a Fourier transform of the dates of observation. The program FTCLEAN was supplied by M. Templeton, written by him based on the CLEAN algorithm of Roberts et al. (1987). The use of this program was first discussed by Templeton & Karovska (2009).

As an example, Figure 3 illustrates the window function for FN Aql, which shows that the frequency space between 1 and 14 years (0.0027 and 0.0002 cycles/day) is reasonably evenly covered.

4.2. Detection Limits

In CRaV we search for Cepheids with orbital velocity variations with an amplitude larger than $1\,\mathrm{km\,s^{-1}}$, that is with a velocity difference between two seasons of at least $2\,\mathrm{km\,s^{-1}}$. In this section we estimate what combinations of mass and period would be detected by this criterion.

We use Monte-Carlo simulations to estimate the fraction of Cepheid companions that will be detected with our method. For each star in our sample we perform the following simulation. We assume a Cepheid mass of $5\,M_{\odot}$ and form a grid of eleven values for the mass of the secondary and 50 logarithmically spaced values for the semimajor axis corresponding to periods between 0.5 and 500 years. For each grid point, we generate an array of 1000 random lines of sight to the system and for each line of sight we calculate the radial velocity of the Cepheid at the actual observation spacing (cadence) for the stars. For systems with a large semimajor axis the orbital period of the system can be much longer than the sequence covered by the observations. In this case, the initial position of the secondary becomes important, since the radial velocity of the Cepheid changes much faster close to periastron than at apastron. Thus, we repeat the simulations for 50 evenly spaced initial positions on an elliptical orbit. We then calculate the fraction of the total simulations for each grid point which predicts a velocity difference between the highest and lowest radial velocity $>2\,\mathrm{km\,s^{-1}}$. We take this as an estimate of the probability of detecting a companion with these system parameters based on the radial velocity of the Cepheid.

The *Kepler* equations for the orbit are solved using the implementation of PyAstronomy[11] that is based on the algorithm of Markley (1995). The code for our Monte-Carlo simulations is implemented as an IPython notebook (Pérez & Granger 2007), which is available as an electronic tar.gz file. In the future, updated versions can be found at https://github.com/hamogu/Cepheids.

We perform this whole set of simulations for each star in our sample twice, once with circular orbits and once with elliptical orbits with $\epsilon = 0.5$. For the given binary parameters, the probability of detecting orbital motion varies between different stars in our sample, because they are observed on different time cadences. We thus average the results over the entire sample. Figure 4 shows a contour map of the averaged detection probabilities. It shows that we are not sensitive to periods below about one year, because the radial velocities used in this study are averaged on an annual basis (Figure 2). However, since observations were typically made over a period of weeks or months, and the shortest orbital periods result in the largest orbital motion, it is unlikely that many systems are missed for orbital periods close to 1 year. Except for very low mass companions, we expect to find almost all binary systems with periods below 10 or 20 years. For higher mass secondaries larger semimajor axes and thus longer periods are detected. Since the estimates are based on the actual years of observation, the best way to increase the detection fraction is to increase the length of the time series, which we plan to do in a future paper.

To confirm that we have selected reasonable parameters for the simulation and also aid in the analysis below, we have compiled a list of stars with orbits. The list began with the list assembled by Szabados[12] and includes orbits from Groenewegen (2013). We have made no attempt to improve orbits, only to select one which gives reliable parameters. Figures 5 and 6 are from this list of Cepheids with orbits (U Aql, FF Aql, V496 Aql, RX Cam, Y Car, YZ Car, DL Cas, XX Cen, MU Cep, AX Cir, SU Cyg, VZ Cyg, MW Cyg, V1334 Cyg, Z Lac, S Mus, AW Per, S Sge, W Sgr, V350 Sgr, V636 Sco, αUMi, FN Vel, and U Vul). The eccentricity values in the simulation cover essentially the full range observed in the orbits.

[11] http://www.hs.uni-hamburg.de/DE/Ins/Per/Czesla/PyA/PyA/index.html
[12] http://www.konkoly.hu/CEP/orbit.html

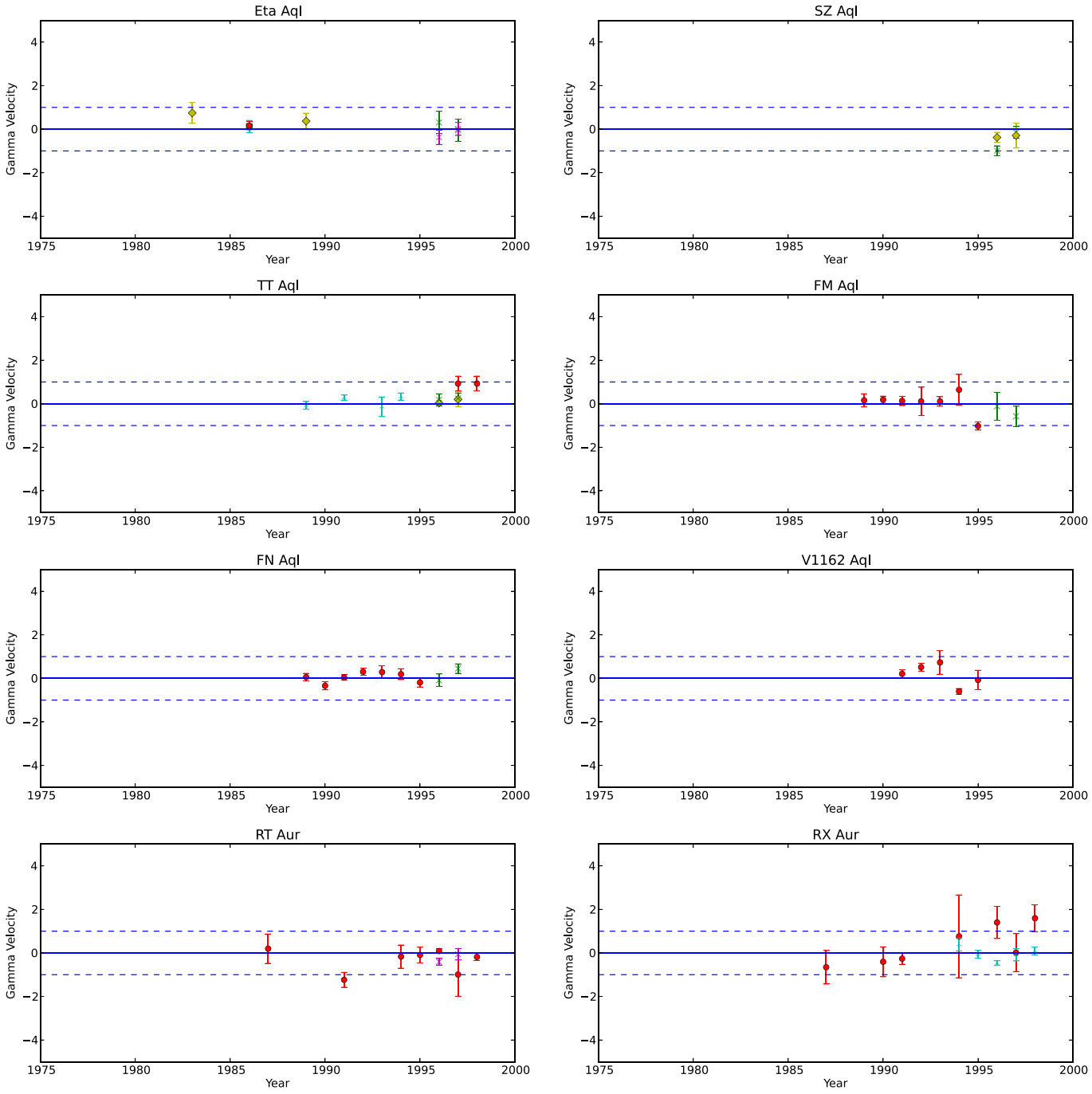

Figure 2. Annual mean radial velocities corrected for pulsation by year. Symbols for the data sources are listed in Table 1. All velocities are in km s^{-1}. Dashed lines show ± 1 km s^{-1}.

5. DISCUSSION

5.1. Binary Frequency

We have now derived annual mean velocities from the large quantity of accurate velocity measures for Cepheids (Figure 2). Because of the challenges of maintaining velocity zero points over 20 years, as well removing the pulsation velocities sometimes in the face of variation in pulsation periods, we use the following criterion to assess the results. Annual means that are within 1σ of the ± 1 km s^{-1} band in Figure 2 are considered to show *no* orbital variation. This judgement was confirmed by the fact that in several instances, two sets of observations from different instruments were made during a single year. Typically they are both located within the band, or very occasionally, when one set is outside the band, the other is within it, hence indicating no variation. (In Figure 2, we only include years with more than 1 observation.) That limit is realistic, but means that we would not identify orbital motion with an amplitude less than 1 km s^{-1}. In addition, in the analysis for binaries (below) we omitted stars with less than 4 years of observations (SZ Aql, Y Oph, and CK Cam).

The star showing the largest indication of orbital motion in Figure 2 is δ Cep itself. This suggests putting it on a watch list. However, there are a number of previous high resolution

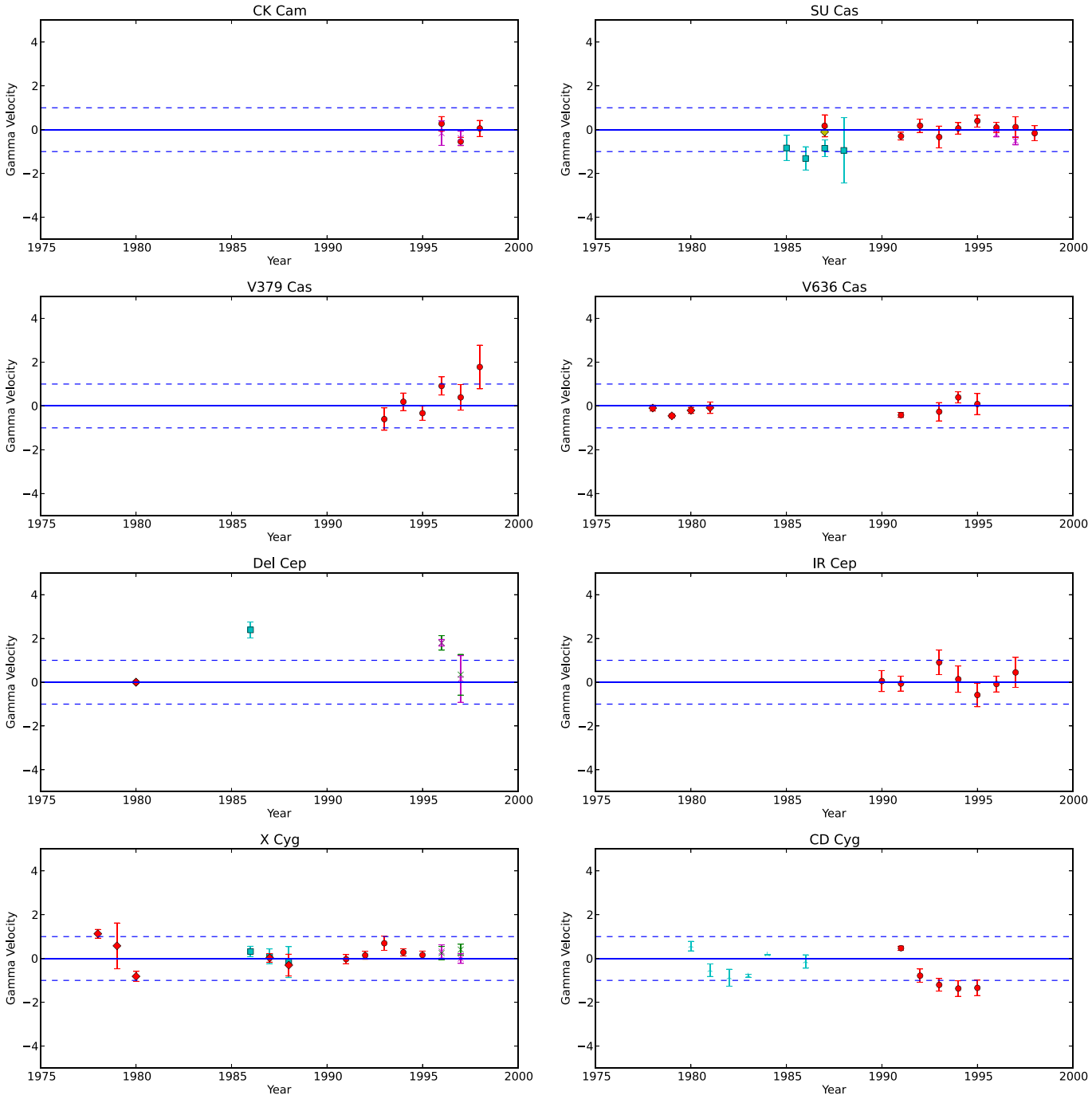

Figure 2. (Continued.)

spectral studies of δ Cep for further comparison. Specifically, Shane (1958) discusses three sets of spectra taken with the Mills three prism spectrograph at Lick Observatory (10 Å mm^{-1} at 4500 Å) in 1907, 1923, and 1950, all providing good phase coverage (Table 5). All three series have a mean velocity within 0.1 km s^{-1} of the mean of −16.1 km s^{-1}. There is a further 10 Å mm^{-1} series from Dominion Astrophysical Observatory in 1975–1978 (Wallerstein 1979). He finds them to have the same systemic velocity within the errors. We have also determined the systemic velocity directly for Bersier et al. (1994), Barnes et al. (2005), Storm et al. (2004), and Kiss & Vinko (2000) in the same way as described for SV Vul and S Vul in the Appendix, all compiled in Table 5. Bersier data is the most negative, as shown in Figure 2, but the spread is only about 2 km s^{-1}, our detection interval.

After the completion of the discussion above, Anderson et al. (2015) presented new high precision radial velocities (0.015 km s^{-1}) for δ Cep. They concluded that it is a binary with an amplitude of 1.5 km s^{-1}, a period of 6.0 years, and a high eccentricity (0.647). We had concluded there is little evidence for orbital motion beyond our survey goal of $\pm$1 km s^{-1}. The new results, particularly the low amplitude and large eccentricity, mean it is not surprising that additional very high quality data was needed for a confident orbital

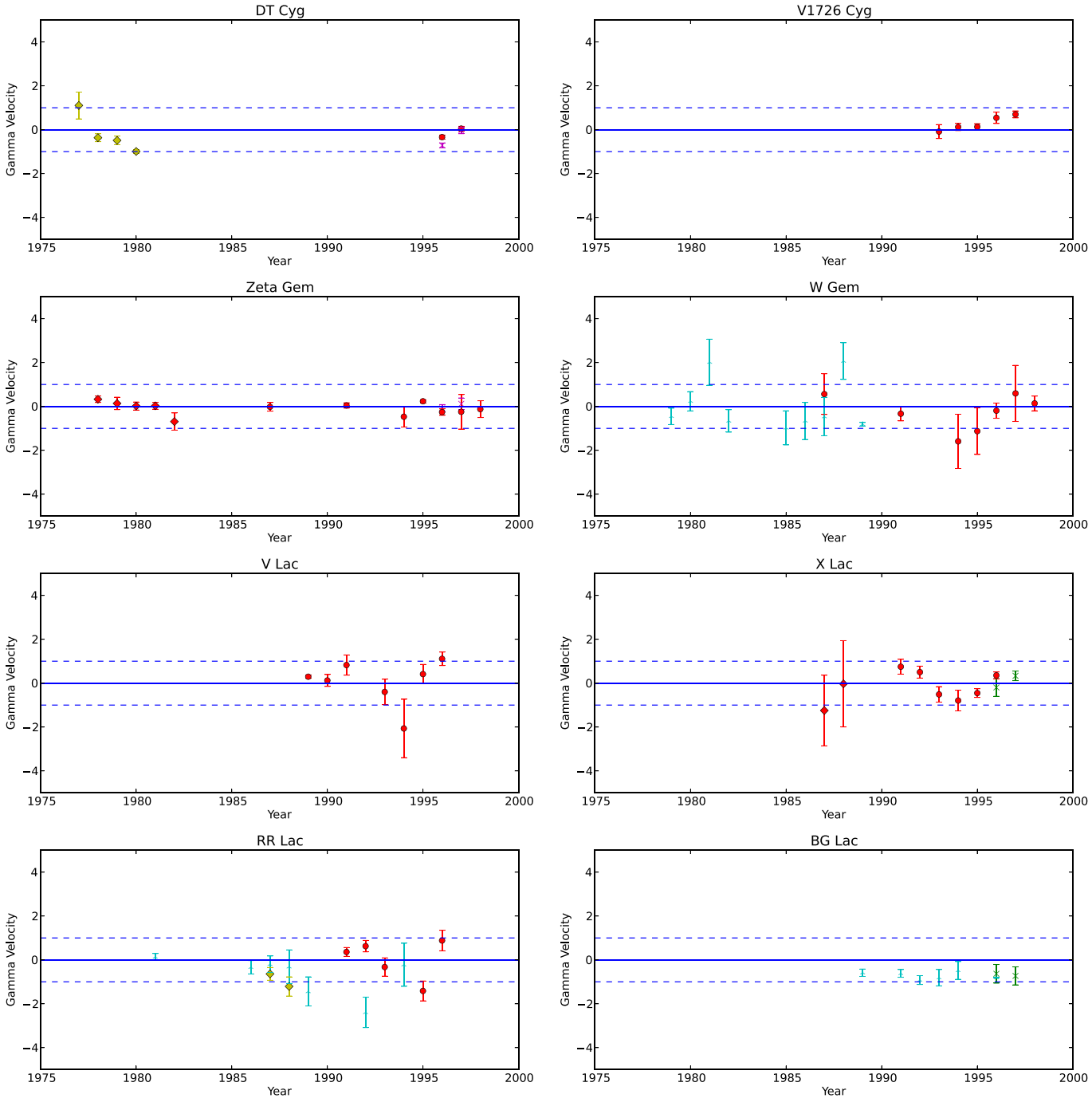

Figure 2. (Continued.)

detection. (We have retained the non-binary listing in Table 6 and the statistics.) More important, this serves to emphasize that our binary frequency is only an upper limit because other low amplitude systems no doubt remain undetected.

We have proceeded as follows to assess the fraction of binaries among Cepheids. From the Cepheid database[13] we have generated a list of Cepheids north of −20°.9, and ordered them by decreasing luminosity (Table 6). None of the Cepheids in the current study were found to have orbital motion with an amplitude larger than 1 km s^{-1}, and these stars have been marked with an x in Table 6. Three stars with observations spanning less than 4 years (SZ Aql, Y Oph, and CK Cam) are considered to have insufficient velocities, and left blank in the table. On the other hand, stars known to be binaries showing orbital motion are marked "bin" in the table. References are given in the Konkoly Cepheid orbit table.[14]

[13] http://www.astro.utoronto.ca/DDO/research/cepheids/

[14] http://www.konkoly.hu/CEP/orbit.html

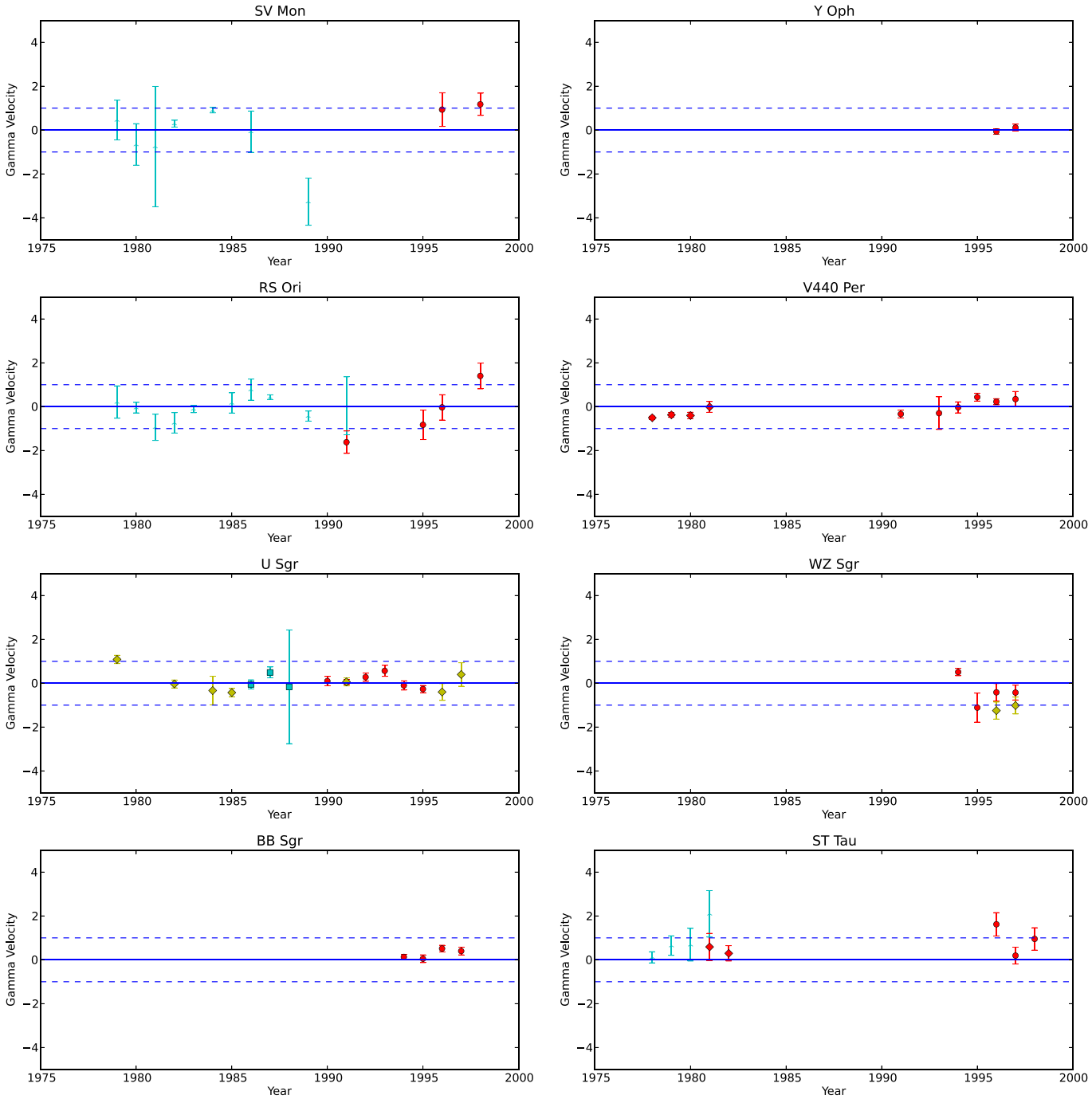

Figure 2. (Continued.)

Several designations in Table 6 need additional discussion. V496 Aql and VZ Cyg have orbits from Groenewegen (2013). X Pup and XX Sgr have recently been discussed by Szabados et al. (2012), and they postulate low amplitude orbital motion in both. For X Pup, recent data shows little change in velocity. Among the older data, we have deferred the velocities from Caldwell et al. (2001) to a later paper in order to cross check against other southern stars. Thus, we leave the X Pup blank (unknown) in Table 6, however future analysis and observations may lead to reclassification. For XX Sgr, the data during the era of the current project indicate no orbital motion. Only older data at lower dispersion (Joy 1937) have discordant velocities. Again, it is listed as blank (unknown) in Table 6. V1344 Aql ($V = 7.77$ mag) has been examined for orbital motion by Szabados et al. (2014). Data from the era of the current project shows essentially no variation, and even older data shows only very small radial velocity shifts, so we classify this star as unknown in Table 6.

Because the quantity and quality of data often decreases for fainter stars, we have adopted the following strategy to assess the results. We have ordered the Cepheids from the brightest to the faintest (Table 6). We have divided the data into three groups of $\simeq$20 stars in this list and derived the binary fraction for each group separately. Table 7 contains the results. The first

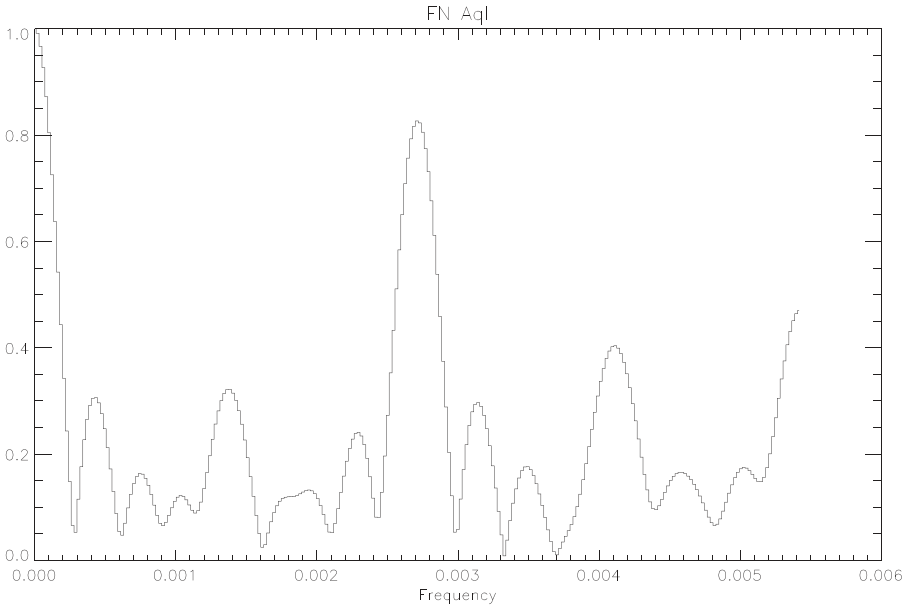

Figure 3. Window function for FN Aql. Frequency is in cycles/day. The period of interest (1–14 years or 0.0027 and 0.0002 cycles/day) is reasonably well covered.

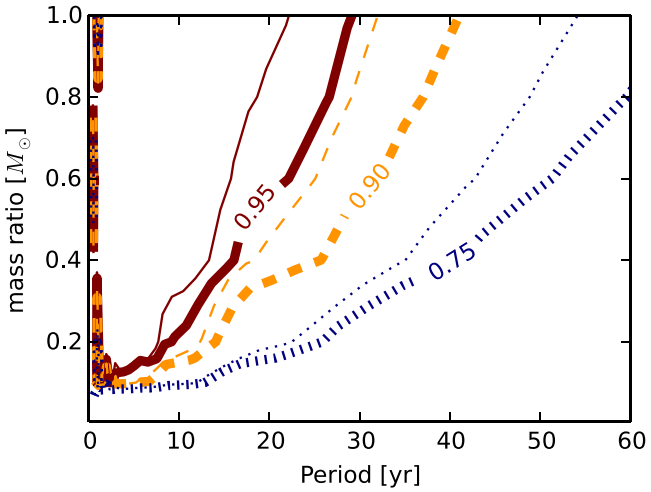

Figure 4. Probability of detecting the binary companion of a Cepheid based on the radial velocity of the primary. The simulations assume that a radial velocity difference >2 km s^{-1} leads to a significant detection. Further assumptions are discussed in the text. The thick lines are contours of the detection probability for circular orbits, the thin lines for elliptical orbits with $\epsilon = 0.5$. The value of the detection probability for the circular orbits is labeled in the plot; the labels also apply to the thin lines of equal color and line style.

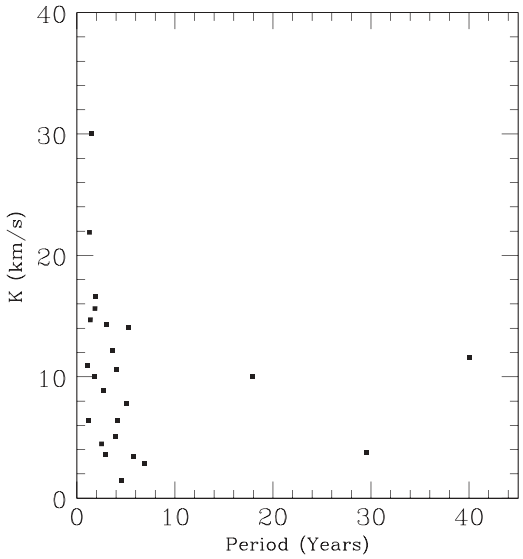

Figure 5. Orbital velocity amplitude of Cepheid orbits as a function of the orbital period.

3 rows are for the groups, with the magnitude range of the stars in Column 2. Columns 3, 4, and 5 contain the number of stars for which velocities are available in our sample, the number of binaries in the group and the fraction which are binaries respectively. We have estimated the uncertainty in the ratios using Equation (1) from Alcock et al. (2003). The final column shows the percentage of the group which was sampled in the top section of the table. (In the bottom half where a subset of the data is discussed, it is omitted.) The final row gives the results for the whole sample. We have retain the classification of δ Cep as single (which we originally concluded). Adding it to the binary group (Anderson et al. 2015) would raise the binary fraction for the brightest 20 stars to 42%.

As can be seen in Table 7 (top), the percentage of binaries *appears* to decrease as the groups become fainter. We consider this to be only an indication of the difficulty in detecting binary motion in the fainter sample, however it alerts us to a possible selection effect. A similar decrease in apparent binary fraction for fainter stars for all period/separation ranges was found by Szabados (2003). The three groups, however, give the same fraction within the 1σ errors. The two groups of the brightest stars give very close results, within 0.2σ. Combining them, we get a binary fraction of $35\% \pm 8\%$. Comparing this with the binary fraction from the faintest group provides weak statistical evidence of a selection effect in fainter stars,

We want to consider a further refinement to the statistics in Table 7. In the final column in Table 6 we have added the orbital period from Table 8. Since the velocity studies in this project (Table 7) cover the range of 1–20 years, the bottom of

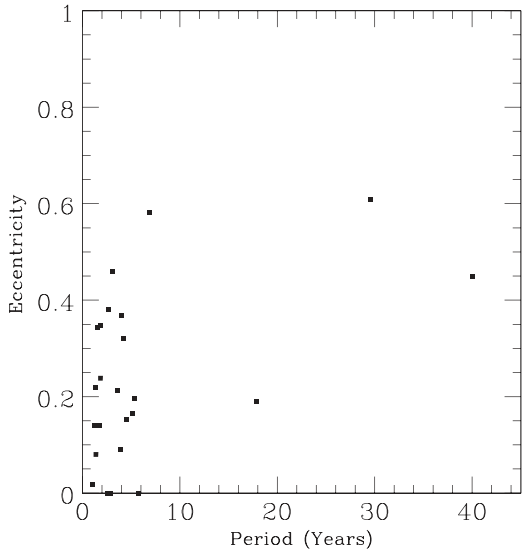

Figure 6. Orbital eccentricity of Cepheid orbits as a function of orbital period.

Table 5
δ Cep Velocities

Year (approx.)	Sys. Vel $\pm \sigma$ (km s^{-1})	Source
1907	-16.1 ± 0.1	Shane (1958)
1923	-16.2 ± 0.1	Shane (1958)
1950	-16.1 ± 0.1	Shane (1958)
1977	−16.	Wallerstein (1979)
1980	-17.4 ± 0.1	Bersier et al. (1994)
1986	-15.3 ± 0.2	Storm et al. (2004)
1996	-15.9 ± 0.1	Barnes et al. (2005)
1996	-15.6 ± 0.1	Kiss & Vinko (2000)

Table 7 shows the statistics when binaries with longer periods are omitted. Again, the results from the two brightest groups are very similar. Combining them, we get a binary fraction of $29\% \pm 8\%$ ($20\% \pm 6\%$ per decade of orbital period), which becomes our preferred fraction.

Determining the frequency of binaries/multiples for intermediate mass stars in the period range 1–20 years is the aim of this study. As discussed in the introduction, this radial velocity study is part of a group of three studies, including an *HST* study of resolved companions and an X-ray study of low mass companions of B stars. The sample of spectroscopic binaries containing Cepheids includes systems with separations of approximately 2–13 AU. Thus, the binary frequency derived here (29%) pertains to only part of the whole range of separations. A more comprehensive value for binary fraction will be discussed in the study of resolved companions. In this section, we will compare our result with those of other studies.

O Stars: A number of recent studies have discussed the massive O stars. Mason et al. (2009) found 30% of O stars to be spectroscopic binaries (excluding their questionable spectroscopic binaries) which rises to 75% when visual companions are included. This, of course includes shorter orbital periods than the present study, down to a few days. Thus the higher radial velocity accuracy of Cepheids and the resulting binary frequency of 29% for only periods of 1–20 years implies a significantly larger fraction of spectroscopic binaries for the

Table 6
Multiplicity Status

Star	$\langle V \rangle$ (mag)	$P_{\rm pulsation}$ (d)	Status[a]	$P_{\rm orbit}$ (year)
Alp UMi	1.982	3.970	bin	29.6
Eta Aql	3.897	7.177	x	⋯
Zeta Gem	3.918	10.151	x	⋯
Del Cep	3.954	5.366	x	⋯
FF Aql	5.372	4.471	bin	3.9
RT Aur	5.446	3.728	x	⋯
S Sge	5.622	8.382	bin	1.9
T Vul	5.754	4.435	x	⋯
DT Cyg	5.774	2.499	x	⋯
V1334 Cyg	5.871	3.333	bin	5.3
SU Cas	5.970	1.949	x	⋯
T Mon	6.124	27.025	bin	$\geqslant 90$
Y Oph	6.169	17.127	⋯	⋯
V440 Per	6.282	7.570	x	⋯
X Cyg	6.391	16.386	x	⋯
U Aql	6.446	7.024	bin	5.1
SZ Tau	6.531	3.148	x	⋯
U Sgr	6.695	6.745	x	⋯
SU Cyg	6.859	3.845	bin	1.5
BB Sgr	6.947	6.637	x	⋯
W Gem	6.950	7.914	x	⋯
U Vul	7.128	7.991	bin	6.9
TT Aql	7.141	13.755	x	⋯
V636 Cas	7.199	8.377	x	⋯
SV Vul	7.220	44.995	x	⋯
YZ Sgr	7.358	9.554	⋯	⋯
V350 Sgr	7.483	5.154	bin	4.0
AW Per	7.492	6.464	bin	40.0
CK Cam	7.58	3.295	⋯	⋯
RX Aur	7.655	11.624	x	⋯
RX Cam	7.682	7.912	bin	3.1
V496 Aql	7.751	6.807	bin	2.9
V1344 Aql	7.767	7.478	⋯	⋯
IR Cep	7.784	2.114	x	⋯
V1162 Aql	7.798	5.376	x	⋯
WZ Sgr	8.030	21.850	x	⋯
EU Tau	8.093	2.102	x	⋯
RY CMa	8.110	4.678	⋯	⋯
SS Sct	8.211	3.671	⋯	⋯
ST Tau	8.217	4.034	x	⋯
SV Mon	8.219	15.233	x	⋯
FM Aql	8.270	6.114	x	⋯
FN Aql	8.382	9.482	x	⋯
X Lac	8.407	5.445	x	⋯
RS Ori	8.412	7.567	x	⋯
Z Lac	8.415	10.886	bin	1.0
X Pup	8.460	25.961	⋯	⋯
V526 Mon	8.597	2.675	x	⋯
SZ Aql	8.599	17.141	⋯	⋯
RW Cam	8.691	16.415	⋯	⋯
RR Lac	8.848	6.416	x	⋯
X Vul	8.849	6.320	x	⋯
XX Sgr	8.852	6.424	⋯	⋯
BG Lac	8.883	5.332	x	⋯
V Lac	8.936	4.983	x	⋯
CD Cyg	8.947	17.074	x	⋯
VZ Cyg	8.959	4.864	bin	5.7
S Vul	8.962	68.464	x	⋯
GQ Ori	8.965	8.616	⋯	⋯
DL Cas	8.969	8.001	bin	1.9
V379 Cas	9.053	4.306	x	⋯

Note.
[a] bin—binary; x—single.

Table 7
Binary Fraction

Star # Table 6	$\langle V \rangle$ mag	# Single Table 4	# Binary Table 6	% Binary	% Sample
			$P_{\rm orbit} > 1$ year		
1–20	<6.9	12	7	37 ± 11	19/20 = 95%
21–40	6.9–8.2	10	5	33 ± 12	15/20 = 75%
41–61	8.2–9.0	13	3	19 ± 10	16/21 = 76%
Total	···	35	15	30 ± 7	50/61 = 82%
			$P_{\rm orbit}$1−20 year		
1–20	<6.9	12	5	29 ± 11	···
21–40	6.9–8.2	10	4	29 ± 12	···
41–61	8.2 –9.0	13	3	19 ± 10	···
Total	···	35	12	26 ± 6	···

Table 8
Mass Ratios

Star	M_2 ($M_\odot$)	M_1 ($M_\odot$)	q	$P_{\rm pulsation}$ (d)	Ref	$P_{\rm orbit}$ (year)
SU Cyg	3.2	4.7	0.68	3.845	1	1.5
α UMi	1.26	4.7	0.27	3.970	3	29.6
FF Aql	1.6–1.4	4.9	0.31	4.471	2	3.9
Y Car	2.5	4.9	0.51	4.640	2	2.7
V1334 Cyg	4.0	4.9	0.82	4.722	1	5.3
V350 Sgr	2.5	5.1	0.49	5.154	1	4.0
AX Cir	5.0	5.2	0.96	5.273	1	17.9
AW Per	4.0	5.4	0.74	6.464	1	40.0
V636 Sco	2.4	5.6	0.43	6.797	1	3.6
V496 Aql	<1.9	5.6	<0.34	6.807	4	2.9
U Aql	2.3	5.7	0.40	7.024	1	5.1
W Sgr	<2.2	5.8	<0.38	7.595	1	4.5
RX Cam	2.2	5.8	0.38	7.912	1	3.1
U Vul	<2.1	5.8	<0.36	7.991	4	6.9
DL Cas	2.5	5.8	0.43	8.001	2	1.9
S Sge	1.7–1.5	5.9	0.27	8.382	2	1.9
S Mus	5.3	6.2	0.85	9.660	1	1.4
Z Lac	<1.9	6.4	<0.30	10.886	2	1.0
XX Cen	<2.1	6.5	<0.32	10.953	2	2.5
YZ Car	<2.9–2.2	7.7	<0.32	18.166	2	1.8
MU Cep	···	···	···	3.768	···	4.2
VZ Cyg	···	···	···	4.864	···	5.7
FN Vel	···	···	···	5.324	···	1.3
MW Cyg	···	···	···	5.955	···	1.2

References. (1) Evans et al. (2013), (2) Evans (1995) + $M_{\rm Cep}$, (3) Evans et al. (2008), (4) Evans (1992) + $M_{\rm Cep}$.

whole period range of the progenitor population of main sequence B stars. Sana & Evans (2011) find a spectroscopic binary fraction from Milky Way open clusters for O stars of 44% over the whole range of periods. Since only about ≃15% of these (their Figure 3) have periods longer than a year, again, our binary fraction 29% over this period range implies a larger percentage over the entire period range. Alternately, the binary fraction of Sana & Evans (2011) for periods less than a year becomes 37%. This would be added to the binary fraction we find for periods longer than a year, resulting in 66% for the whole period range.

Kobulnicky et al. (2014) report on a sample of 48 O and early B stars in the Cyg OB association including binaries with periods up to 5000 days. They combine their results with those of Sana et al. (2012) and Garmany et al. (1980). They stress the large incompleteness factor they derive for the longer periods, the period range covered in the present study. In fact, the results of our study nicely confirm the incompleteness corrections they derive. For instance, if the 29% binary fraction we derive for the period range 1–20 years (log P = 2.6–3.9 for P in days) is added to the cumulative fraction as a function of period (their Figure 31), the binarity fraction reaches ≃60%, close to their estimated total. Again, the period range covered by the Cepheid sample and the high level of completeness (Figure 4) underscores the value of the Cepheid velocities. Caballero-Nieves et al. (2014) have performed a survey of OB stars in the Cyg OB association with the *HST* Fine Guidance System and find resolved companions as close as 23 mas. They find a binary frequency of 22%–26% in the period range 20–20,000 years, the period range immediately larger than that of the Cepheid sample. They have the important result that this frequency establishes a downturn in the frequency as a function of period, as also found by Evans et al. (2013) for Cepheid systems with mass ratios ⩾0.4.

B Stars: Several recent studies have been done of stars about the same mass as the Cepheids. Chini et al. (2012) break their spectroscopic survey down into smaller spectral type bins. Their O3 to B1.5 group has a spectroscopic binary frequency of approximately 70%. Their B2 to B6 group corresponds to the mass range of the Cepheid sample (Table 7), and the binary frequency has fallen to approximately 50%. For their lower mass B stars (B7, B8, B9), the frequency is approximately 15%. Again, the Cepheid frequency of 29% for the limited period range implies a higher frequency than the B7, B8, B9 stars for the whole period range. Abt, Gomez, and Levy discussed B2 to B5 stars. Thirty two of their sample of 109 (29%) were actually observed to have orbital motion. They made a correction for incompleteness which increased the fraction to 59%. The radial velocity sample, however, was only sensitive to periods less than a year. That fraction should be added to the fraction in the Cepheid sample, where only periods longer than a year are found.

A Stars: For stars slightly less massive than Cepheids, two recent studies have provided results: De Rosa et al. (2014) and Kouwenhoven et al. (2007). De Rosa et al. (2014) found a multiplicity fraction of ⩾44% from a combined spectroscopic and imaging survey over the full period range for a volume limited sample of A stars. Again, the binary fraction from the limited period range of the Cepheids implies a larger total binary fraction. Kouwenhoven et al. (2007) analyzed the binary frequency for intermediate mass stars in Sco OB2. They used the spectroscopic observations of Levato et al. (1987), and found 30% of the sample of 53 binaries with orbits. Again, all the orbits have periods (much) less than a year. This fraction thus should be added to the Cepheid fraction. They found a further 43% to have variable radial velocities. At least some of these are low amplitude binaries, however some of them may be variable because of pulsation. Kouwenhoven et al. also discussed the spectroscopic observations of Brown & Verschueren (1997). For their sample of 71 stars, 24% are spectroscopic binaries. A further 39% have variable radial velocities, again likely to be divided between orbital motion and pulsation.

G Stars: For solar mass stars, the most recent determination comes from Raghavan et al. (2010), who found a multiplicity frequency of 44%. Because these stars are nearby and sharp-lined, the corrections for incompleteness are much smaller than for more massive stars. Thus, the current study as well as other studies above confirm a smaller multiplicity fraction than for more massive stars.

Thus, this survey of Cepheid velocities in the period range of 1–20 years finds a binary frequency which consistently implies a higher frequency (at all period ranges) than found in studies of main sequence stars. This is reasonable because of the high accuracy of the Cepheid velocities compared with other massive stars. The periods discussed here are longer than typically investigated in the main sequence studies, which is exactly where the orbital velocities are smaller, and hence companions of main sequence stars will be missed. Presumably a large fraction of short period binaries would be discovered in the main sequence studies, but the velocity accuracy of this study is required to find the longer period systems. Thus, we stress that the Cepheid sample fills in the period range between the short periods usually detected in massive star studies and the long periods of resolved companions.

Neilson et al. (2015) compared the fraction of Cepheids in spectroscopic binaries with a binary population synthesis model, and found generally good agreement. The number favored here has been slightly revised from the fraction they used (35%), but the general agreement still holds.

As mentioned above, there are two very important effects which modify the binary fraction in the Cepheid sample: dynamical evolution and mergers/binary interaction. Any system with more than two stars may be unstable to dynamical interaction between the components which sometimes leads to the ejection of one star (typically the smallest). This study provides no information about this topic. The second effect was discussed by Sana et al. (2012) who concluded that three quarters of all O stars will either merge (20%–30%) or have interactions resulting in stripping the envelope or accreting mass because of Roche lobe overflow as they evolve off the main sequence. Binaries in the Cepheid sample (Table 8) may have suffered no consequences from this. However, there may be some systems in the list of single stars (Table 6) which began life as a short period binary, but have now merged, thus moving from the binary list to the single list. The obvious and simplest result of this is to increase the number of currently single stars and decrease the binary fraction.

5.2. Mass Ratios

We have stressed that Cepheids provide a well characterized sample to investigate the properties of spectroscopic binaries, specifically, in the period range of 1–20 years. In addition to providing the binary frequency, this group has another valuable property. Because the primary (Cepheid) has evolved to become a cool supergiant, hot companions can be observed directly in the ultraviolet. Ultraviolet spectra, specifically from the *International Ultraviolet Explorer* (*IUE*) satellite, provide either an uncontaminated spectrum of the companion or an upper limit. Thus the temperature can be directly observed, and from that a mass inferred. We have derived masses for the companions in this way in Table 8. The sample used is the sample of stars with orbits (including both N and S hemispheres.) Masses of the companion (Table 8, Column 2) are taken from Evans et al. (2013), the *IUE* survey (Evans 1995), or the *HST* measurement of Polaris (Evans et al. 2008), as indicated in Column 6. Masses for the Cepheids (Column 3) are derived as in Evans et al. (2013), using the Leavitt law (period–luminosity relation) from Benedict et al. (2007) and the mass–luminosity relation based on the models of Prada Moroni et al. (2012) with moderate convective overshoot. The periods of the overtone pulsators (αUMi and V1334 Cyg) have been "fundamentalized" for the mass calculation. Mass ratios, $q = M_2/M_1$ (Column 4) are calculated from the Cepheid and companion masses. When a companion mass has a range, a mass from the center of the range was used.

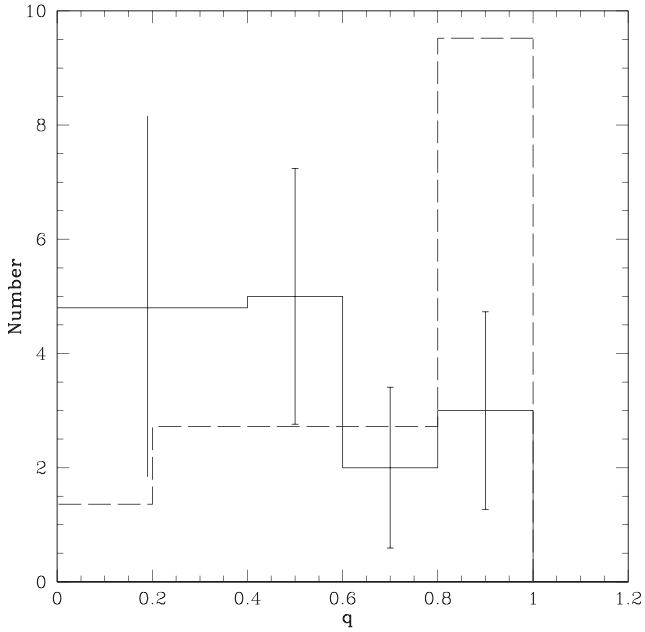

Figure 7. Distribution of mass ratios. Solid line: Cepheids; dashed line: solar mass stars (Raghavan et al. 2010), scaled as described in the text.

A few stars require extra comments. MU Cep, MW Cyg, VZ Cyg, and FN Vel were not observed by *IUE* because they are fainter than the survey limit, so they lack mass ratio information, and are listed at the bottom of Table 8.

The mass ratio data concentrates on orbital periods of 30 years or less because that includes the most of the known orbits, and also corresponds reasonably well to the period range which the present radial velocity data are sensitive to. However, AW Per with a slightly longer orbital period is included. We also made an exception and included W Sgr, even though the mass of the hottest companion (Column 2) is actually of a resolved companion, not the companion of the spectroscopic orbit (Evans et al. 2009). This means the mass ratio is actually an upper limit to the ratio of the spectroscopic system.

Figure 7 shows the distribution of the mass ratios for the Cepheid systems. The q data from Table 8 were divided into bins of 0.2 for $q > 0.4$. For smaller q values (both observed values and upper limits), the data was summed in one q bin 0.0 to 0.4 (total count of 10). The location of the data for the lowest q value is shifted slightly for clarity. Poisson errors are shown. Although the sample is fairly small, it is clear that there is no preference for equal mass companions in the Cepheid sample. We stress that this sample contains systems with periods longer than a year, so this says nothing about studies of shorter period systems which have been found in some studies to show a

preference for equal mass companions. Creating a single bin for stars with $q < 0.4$ may disguise a rise in frequency for small q values. If even half of the 6 stars which have only an upper limit belong to the 0.2–0.4 bin, the number in that bin rises to 7, larger than the 0.4–0.6 bin. Even with a simpler division into two bins, 0–0.5 and 0.5–1.0 because of small number statistics, the result still favors small q systems. The two bins have 14 and 6 systems, respectively. In addition, from the detection analysis (Figure 4), any undiscovered binaries are likely to be in the 0.0–0.2 bin. Nevertheless, the mass ratio distribution is relatively flat, and similar to that found by Sana & Evans (2011) for more massive O stars over the whole range of periods they studied.

As we get more and more information about binary/multiple systems, we can investigate the finer detail of the properties. We have used the data of Raghavan et al. (2010) to create a comparison with solar mass stars. Specifically, we have used their Figure 17 (the spectroscopic binaries shown as +) to create a distribution of mass ratios for the period range 1–30 years. This is shown in Figure 7 for comparison, scaled by the size of the sample. The mass ratio distribution for the solar mass stars is relatively flat for $q < 0.8$. similar to that for the Cepheids. For larger q, the solar mass stars have a much larger fraction of equal mass pairs than the Cepheids.

The purpose of CRaV, and other studies of binary properties is to identify characteristics which relate to star formation, and how properties vary depending on the stellar mass, and the separation of the systems. In the comparison in Figure 7 between 5 $M_{\odot}$ Cepheids and solar mass stars, it may be that the apparent differences are the result of asking the wrong question. For instance, the companions are also drawn from very different populations (typically 3 $M_{\odot}$ versus 0.5 $M_{\odot}$). From the Figure 17 in Raghavan et al. (2010) it is clear that the distribution of q changes from short period systems (large q) to longer period ones (spread in q to smaller values). In this sense, the distribution of q for solar mass stars would be more similar for the group of longer period stars.

A brief comparison with the previous distribution of mass ratios for Cepheids (Evans 1995) is in order. The current distribution of q is flatter for two reasons. First, accumulating evidence favors somewhat smaller Cepheid masses. Second, a realization of the large number of triple systems makes the derivation of lower limits more questionable.

One further point should be mentioned in discussing the binary fraction of Cepheids. In addition to the alteration in the binary systems when a post-main sequence short period binary undergoes Roche lobe overflow, there may be mass loss during the Cepheid phase itself. See, for example the summary in Neilson et al. (2012). While mass loss at this phase is not as dramatic as in massive main sequence stars, it could affect both the mass ratios and the orbits. In addition, comparison with main sequence progenitors will be altered. Resolution of these questions awaits further information on mass-loss at the Cepheid phase.

6. SUMMARY

We have examined velocity data for 35 Cepheids to determine the binary/multiple fraction. The velocity data have a typical accuracy of 1 km s^{-1} per observation, and were obtained over a period of 20 years. After correcting the observed velocities for the pulsation velocity, annual means were formed. We have assessed our detection limits and found a high probability of recognizing binary systems with mass ratios as small as 0.1 and periods as long as 20 years. Further data extending the time series will increase the the period/separation range. A binary fraction was formed by combining this sample with Cepheids known to be members of binary/multiple systems. The binary fraction appears to decease at fainter magnitudes. However, we take this to be an indication of undiscovered binaries at fainter magnitudes. Therefore, we conclude that the most reliable binary fraction of $29\% \pm 8\%$ ($20\% \pm 6\%$ per decade of orbital period) comes from the sample of the 40 brightest stars, which has the most complete information. The range of separations that the Cepheids sample probes is approximately 2–20 AU, which is poorly studied for other massive stars. Comparing the binary fraction in this limited period/separation range with the other recent determinations of binary frequency confirms that the high accuracy velocities of the Cepheids results in a higher binary frequency. The distribution of the mass ratio q is also examined from spectral information about the companions in the ultraviolet, and found to be flat as a function of q.

Future work is planned to extend the time span in the northern hemisphere, and also to make a similar analysis of Cepheids in the southern hemisphere.

We are grateful for comments from A. Tokivinin and B. Mason which resulted in an improved manuscript. It is a pleasure to thank Beth Sundheim and Bharath Kumaraswamy for work at the beginning of this project. We also thank Matthew Templeton for providing the program FTCLEAN used to generate the window functions, and for advice on its use. Comments from an anonymous referee improved the presentation of the paper. Support for this work was also provided from the *Chandra* X-ray Center NASA Contract NAS8-03060 and *HST* grant GO-12215.01-A. N.A.G. is grateful to Russian Foundation for Basic Reserach grant No. 14-02-00472 for the support of radial velocity measurements. A.S.R. is grateful to Russian Scientific Foundation grant No. 14-22-0041 for the support of data processing. P.M. acknowledges support from the Polish NCN grant no. DEC-2012/05/B/ST9/03932. Vizier and SIMBAD were used in the preparation of this study.

APPENDIX
PERIOD VARIATIONS

The stars which have period variations more complex than a constant period or a constantly changing period are discussed here, with Figures showing the "$O - C$" (Observed minus Computed) diagrams. The representation in the text and figures is the same for all stars: C is the JD of maximum light, E is the epoch.

A.1 EU Tau

As with many overtone pulsators, EU Tau has erratic period fluctuations (Szabados 1983; Berdnikov et al. 1997; Evans et al. 2015). This is shown in the $O - C$ diagram of recent photometry (Figure 8) for:

$$C = 2445651.13 + 2.1024924 \times E.$$

In the case of EU Tau, the best fit for the time period discussed in this study (which begins just before 2,445,000), is what we

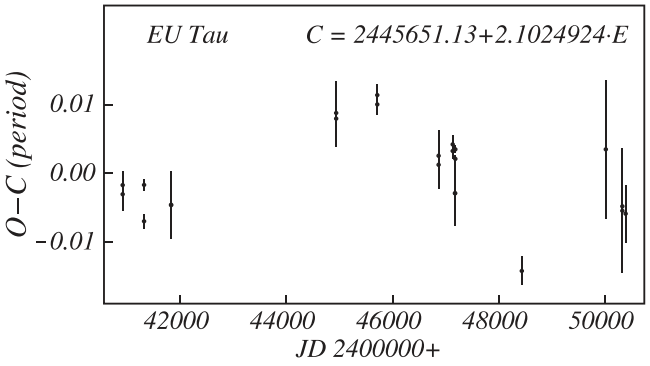

Figure 8. Period variation (Observed minus Computed $O - C$) diagram for EU Tau. Time is in days; $O - C$ is in phase. In the label, C is the computed JD of maximum light; E is the epoch. See appendix for discussion.

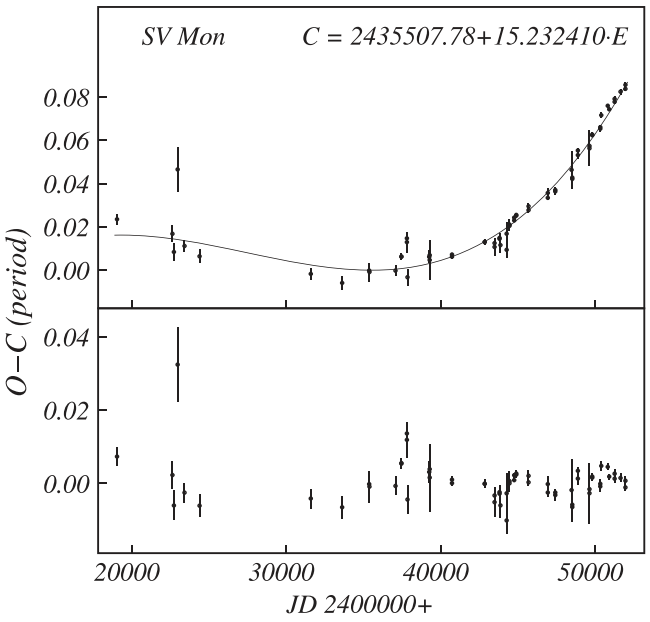

Figure 9. $O - C$ diagram for SV Mon in the same units as Figure 8. Top: data and the cubic fit. Bottom: residuals from the cubic fit.

use to phase the velocity curves together:

$$C = 2449679.541 + 2.10256181 \times E.$$

A.2 SV Mon

SV Mon has a complicated period fitted by Berdnikov with a cubic equation (Figure 9) for the long-term variation:

$$C = 2435507.781 + 15.23241047 \times E + 0.660623600 \times 10^{-6} \times E^2 + 0.415700058 \times 10^{-9} \times E^3.$$

However, for our analysis we used a single period and the Fourier coefficients fitted to the radial velocities

$$C = 2443794.33800 + 15.23278000 \times E.$$

Again this is adequate for the time period covered by the velocities which start just before JD 2,445,000. This star has among the largest errors on the annual means, possibly because of some additional jitter in the period.

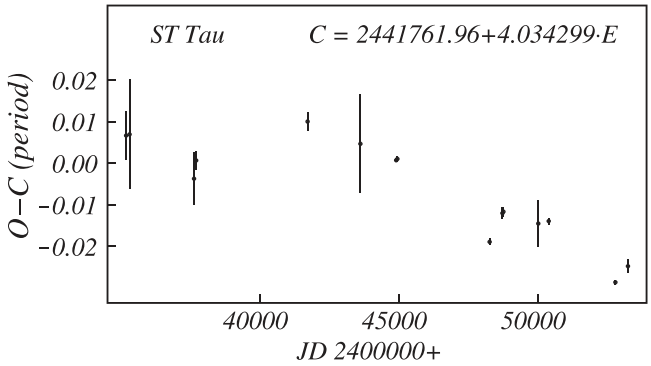

Figure 10. $O - C$ diagram for ST Tau in the same units as Figure 8.

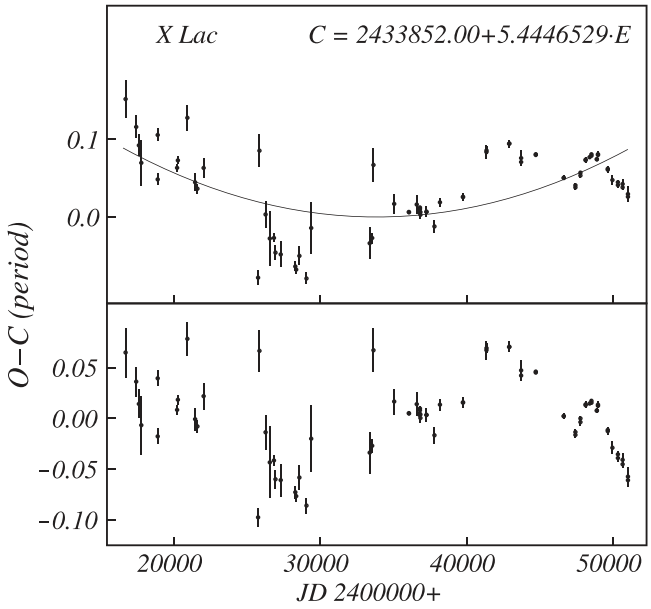

Figure 11. $O - C$ diagram for X Lac in the same units as Figure 8. Top: data plus a parabolic fit; bottom: the residuals from the parabola.

A.3 ST Tau

The period used is from Szabados (1977):

$$C = 2441761.96300 + 4.03429900\, E.$$

This provides a good Fourier series for the velocity curves. The $O - C$ diagram (Figure 10) suggests a possible small period change. Some of the scatter in the resulting plot of the annual mean velocities (Figure 2) is probably due to variations in the period (Figure 10).

A.4 X Lac

The $O - C$ period change diagram for X Lac from photometry is shown in Figure 11. It is evident that the period fluctuations are larger and more erratic than even the parabolic fit can describe. Since the time range covered by velocities is well mapped by photometry, we have approximated the period changes with several linear sections. With this, we have phased together the velocity curves, resulting in Figure 2.

One interesting result of this investigation has been consideration of X Lac. It has a period of 5.4 days and a moderate amplitude (velocity amplitude c(0) in the equation in Section 3.1 is 25 km s^{-1}). These two characteristics do not immediately suggest overtone pulsation, as found in the small

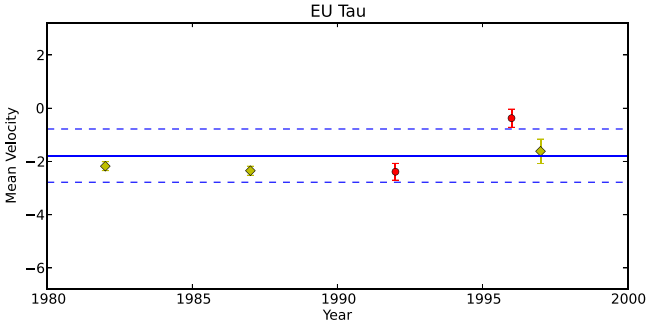

Figure 12. Radial velocities corrected for pulsation (by year) for EU Tau for the fits to the curve without assuming a period (see text). Units and symbols are the same as Figure 2. The results are essentially the same as Figure 2.

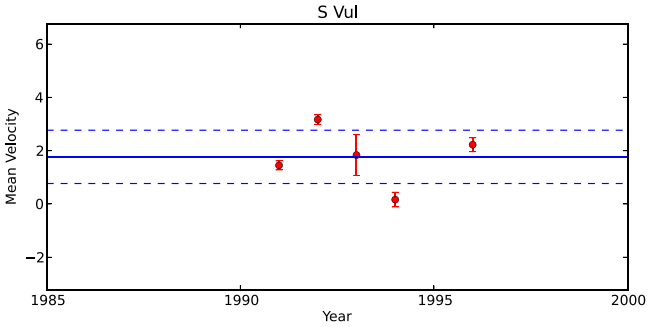

Figure 13. Radial velocities for S Vul corrected for pulsation by year. In this case, data for each year has been fitted individually to annual velocity curves. Units and symbols are the same as Figure 2.

Table 9
Cepheid Annual Mean Velocities: S Vul

JD	Phase	Mean (km s^{-1})	N	Ref	JD Range
48406.65	0.21	1.45	15	Gorynya	47309.46–48565.06
	± 0.002	± 0.17	…	…	…
48886.61	0.22	3.17	22	Gorynya	48795.45–48889.27
	± 0.002	± 0.18	…	…	…
49228.12	0.21	1.84	19	Gorynya	49161.53–49256.32
	± 0.02	± 0.77	…	…	…
49569.13	0.19	0.16	10	Gorynya	49499.52–49609.28
	± 0.004	± 0.27	…	…	…
50117.43	0.20	2.22	21	Gorynya	49926.48–50309.42
	± 0.003	± 0.26	…	…	…

amplitude, short period "s" Cepheids. However, the period varies in an erratic way (Figure 11). Overtone pulsators have unusually large period changes, larger than expected from evolution through the instability strip (Szabados 1983; Berdnikov et al. 1997; Evans et al. 2015). As longer series of photometric data have been accumulated, it appears in many cases that data that was previously fit with a parabola, representing a changing period, is actually a series increasing and decreasing periods. In the case of X Lac the substantial changes in period (Figure 11) raise the interesting question of whether it may in fact be pulsating in the first overtone. The most recent discussion of Fourier diagnostics is given by Storm et al. (2011). In their plot of Fourier amplitude A_1 as a function of period X Lac falls somewhat below the fundamental mode sequence. Similarly, the amplitude ratio R_{21} could be the

Table 10
Cepheid Annual Mean Velocities: SV Vul

JD	Phase	Mean (km s^{-1})	N	Ref	JD Range
43719.09	0.05	−1.67	25	Bersier	43681.59–43735.44
	± 0.001	± 0.16	…	…	…
44393.96	0.04	−3.16	17	Imbert	44168.30–44569.28
	± 0.001	± 0.17	…	…	…
44438.71	0.03	−2.51	30	Bersier	44184.29–44483.40
	± 0.001	± 0.12	…	…	…
44979.86	0.05	−3.56	20	Imbert	44902.29–45139.58
	± 0.002	± 0.22	…	…	…
46692.83	0.11	−2.78	47	Storm	46567.91–46787.53
	± 0.001	± 0.08	…	…	…
47097.69	0.10	−2.48	28	Storm	46842.96–47407.58
	± 0.001	± 0.21	…	…	…
47142.75	0.11	−2.52	17	Bersier	47107.26–47149.29
	± 0.002	± 0.19	…	…	…
47457.08	0.09	−2.95	12	Bersier	47424.32–47495.26
	± 0.001	± 0.19	…	…	…
48537.21	0.09	−2.99	21	Gorynya	48426.52–48600.10
	± 0.002	± 0.17	…	…	…
48851.04	0.06	−2.98	27	Gorynya	48745.52–48921.19
	± 0.002	± 0.16	…	…	…
49210.23	0.04	−3.16	22	Gorynya	49161.54–49256.32
	± 0.004	± 0.36	…	…	…
49569.31	0.02	−3.46	14	Gorynya	49499.54–49609.27
	± 0.002	± 0.45	…	…	…
49973.38	−0.01	−2.87	12	Gorynya	49932.40–50000.24
	± 0.002	± 0.28	…	…	…
50288.13	−0.01	−2.44	15	Gorynya	50236.40–50314.35
	± 0.001	± 0.28	…	…	…
50288.667	−0.004	−1.32	14	Barnes	49947.85–50353.62
	± 0.01	± 0.63	…	…	…
50647.17	−0.04	−2.24	20	Barnes	50609.87–50709.71
	± 0.001	± 0.12	…	…	…

continuation of the overtone sequence as a function of period. The ϕ_{21}-period diagram is more complicated, particularly in the sample discussed by Kienzle et al. (1999). The fundamental and overtone sequences appear to cross near P = 5.44 days, so the value for X Lac provides little information about the pulsation mode. Storm, et al. note that both X Lac and V496 Aql have A_1 and also R_{21} smaller than the fundamental mode sequence. While they find the Fourier parameters inconclusive, the variable period for X Lac is another overtone characteristic, and we tentatively classify it as an overtone pulsator.

What makes this particularly interesting is that there are very few known or suspected overtone pulsators with periods this long. This is partly because some of the standard Fourier diagnostics are ambiguous in this period range. It is therefore valuable to identify possible long period overtone pulsators in order to have a larger sample to define the the overtone locus.

A.5 S Vul

For stars with a variable period, we sometimes resort to the following approach. Instead of taking the phasing of the velocity curves from the period (including a parabolic term as needed) from the photometry, we solve for both the velocity mean and the phase of maximum light from the velocity curve alone. This means we can only use seasons/years with a well defined curve containing many data points. To confirm this approach, the results for EU Tau are shown in Figure 12. The

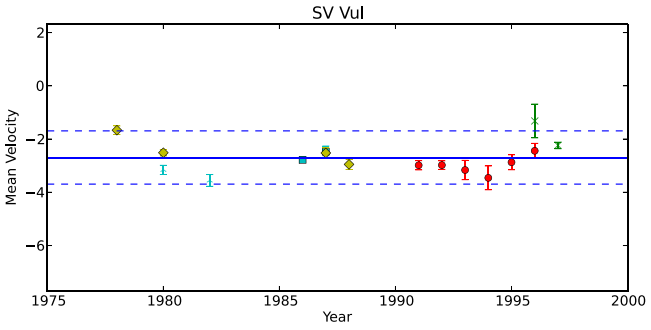

Figure 14. Radial velocities for SV Vul corrected for pulsation by year. In this case, data for each year are from individual fits. Units and symbols are the same as Figure 2.

results are essentially the same as in Figure 2 (with a small mean offset) but with fewer seasons than the standard approach using the photometric period.

S Vul has a period of 68 days with significant period variations (Berdnikov 1994). We have used individual fits to annual velocity curves. Occasionally the means cover more than 1 season, since for this approach, a larger number of data points are needed to do an accurate fitting. Table 9 has the values from these fits which are in shown Figure 13.

A.6 SV Vul

It also has a long period (45 days), and, as with S Vul, we have derived mean velocities by fitting data from individual seasons. Details are given in Table 10 and Figure 14.

REFERENCES

Abt, H. A., Gomez, A. E., & Levy, S. G. 1990, ApJS, 74, 551
Alcock, C., Alves, D. R., Becker, A., et al. 2003, ApJ, 598, 597
Aldoretta, D. J., Caballero-Nieves, S. M., Gies, D. R., et al. 2015, AJ, 149, 26
Anderson, R. I. 2014, A&Ap, 566, 10
Anderson, R. I., Sahlmann, J., Holl, B., et al. 2015, ApJ, 804, 144
Baranne, A., Mayor, M., & Poncet, J. L. 1979, VA, 23, 279
Barnes, T. G., III, Jeffery, E. J., Montemayor, T. J., & Skillen, I. 2005, ApJS, 156, 227
Benedict, G. F., McArthur, B. E., Feast, M. W., et al. 2007, AJ, 133, 1810
Berdnikov, L. N. 1994, AstL, 20, 232
Berdnikov, L. N., Dambis, A. K., & Vozyakova, O. V. 2000, A&ApS, 143, 211
Berdnikov, L. N., Ignatova, V. V., Pastukhova, E. N., & Turner, D. G. 1997, AstL, 23, 177
Bersier, D. 2002, ApJS, 140, 465
Bersier, D., Burki, G., Mayor, M., & Duquennoy, A. 1994, A&ApS, 108, 25
Brown, A. G. A., & Verschueren, W. 1997, A&A, 319, 811
Caballero-Nieves, S. M., Nelan, E. P., Gies, D. R., et al. 2014, AJ, 147, 40
Caldwell, J. A. R., Coulson, I. M., Dean, J. F., & Berdnikov, L. N. 2001, JAD, 7, 4
Chini, R., Hoffmeister, V. H., Nasseri, A., Stahl, O., & Zinnecker, H. 2012, MNRAS, 424, 1925
Coulson, I. M., & Caldwell, J. A. R. 1985, SAAOC, 9, 5
Coulson, I. ,M., Caldwell, J. A. R., & Gieren, W. P. 1985, ApJS, 57, 595
De Rosa, R. J., Patience, J., Wilson, P. A., et al. 2014, MNRAS, 437, 1216
Duchene, G., & Krauss, A. 2013, ARA&A, 51, 269
Duquennoy, A., & Mayor, M. 1991, A&A, 248, 485
Evans, N. R. 1992, ApJ, 384, 220
Evans, N. R. 1995, ApJ, 445, 393
Evans, N. R., Bond, H. E., Schaefer, G. H., et al. 2013, ApJ, 146, 93
Evans, N. R., Carpenter, K., Robinson, R., et al. 1999, ApJ, 524, 379
Evans, N. R., DeGioia-Eastwood, K., Gagne, M., et al. 2011, ApJS, 194, 13
Evans, N. R., Massa, D., & Proffitt, C. 2009, AJ, 137, 3700
Evans, N. R., Schaefer, G. H., Bond, H. E., et al. 2008, ApJ, 136, 1137
Evans, N. R., Szabo, R., Derekas, A., et al. 2015, MNRAS, 446, 4008
Fernie, J. D., Beattie, B., Evans, N. R., & Seager, S. 1995, IBVS, 4148
Freedman, W. L., Hughes, S. M., Madore, B. F., et al. 1994, ApJ, 427, 628
Garmany, C. D., Conti, P. S., & Massey, P. 1980, ApJ, 242, 1063
Gieren, W. P. 1981, ApJS, 46, 287
Gorynya, N. A., Irsmambetova, T. R., Rastorgouev, A. S., & Samus, N. N. 1992, SvAL, 18, 316
Gorynya, N. A., Rastorguev, A. S., & Samus, N. N. 1996, AstL, 22, 175
Gorynya, N. A., Samus, N. N., Sachkov, M. E., et al. 1998, AstL, 24, 815
Groenewegen, M. A. T. 2013, A&Ap, 550, A70
Groenewegen, M. A. T., & Oudmaijer, R. D. 2000, A&A, 356, 849
Imbert, M. 1999, A&ApS, 140, 79
Joy, A. H. 1937, ApJ, 86, 363
Kienzle, F., Moskalik, P., Bersier, D., & Pont, F. 1999, A&Ap, 341, 818
Kimiki, D. C., & Kobulnicky, H. A. 2012, ApJ, 751, 15
Kobulnicky, H. A., Kiminki, D. C., Lundquist, M. J., et al. 2014, ApJS, 213, 34
Kiss, L., & Vinko, J. 2000, MNRAS, 314, 420
Klagyivik, P., & Szabados, L. 2009, A&Ap, 504, 959
Kouwenhoven, M. B. N., Brown, A. G. A., Portegies Zwart, S. F., & Kaper, L. 2007, A&A, 474, 77
Kratter, K. M., & Matzner, C. D. 2006, MNRAS, 373, 1563
Levato, H., Malaroda, S., Morrell, N., & Solivella, G. 1987, ApJS, 64, 487
Markley, F. L. 1995, CeMDA, 63, 101
Mason, B. D., Hartkopf, W. I., Gies, D. R., Henry, T. J., & Helsel, J. W. 2009, AJ, 137, 3358
Neilson, H. R., Langer, N., Engle, S. G., Guinan, E., & Izzard, R. 2012, ApJL, 760, L18
Neilson, H. R., Schneider, F. R. N., Izzard, R. G., Evans, N. R., & Langer, N. 2015, A&A, 574, A2
Pérez, F., & Granger, B. E. 2007, CSE, 9, 21
Petterson, O. K. L., Cottrell, P. L., & Albrow, M. D. 2004, MNRAS, 350, 95
Prada Moroni, P. G., Gennaro, M., Bono, G., et al. 2012, ApJ, 749, 108
Raghavan, D., McAlister, H. A., Henry, T. J., et al. 2010, ApJS, 190, 1
Roberts, D. H., Lehar, J., & Dreher, J. W. 1987, AJ, 93, 968
Sana, H., & Evans, C. J. 2011, in IAU Symp. 272, Active OB stars: Structure, Evolution, Mass Loss, and Critical Limits, ed. C. Neiner, G. Wade, G. Meynet & G. Peters (Cambridge: Cambridge Univ. Press), 474
Sana, H., de Koter, A., de Mink, S. E., et al. 2013, A&A, 550, A107
Sana, H., de Mink, S. E., de Koter, A., et al. 2012, Sci, 337, 444
Shane, W. W. 1958, ApJ, 127, 573
Shatsky, N., & Tokovinin, A. 2002, A&Ap, 382, 92
Storm, J., Carney, B. W., Gieren, W. P., et al. 2004, A&Ap, 415, 531
Storm, J., Gieren, W., Fouqué, P., et al. 2011, A&Ap, 534, A94
Sugars, B. J. A., & Evans, N. R. 1996, AJ, 112, 1670
Szabados, L. 1977, Mitt. Sternw. Ungarish. Akad. Wissensch., 70, 1
Szabados, L. 1983, Ap&SS, 96, 185
Szabados, L. 2003, in ASP Conf 298, GAIA Spectroscopy: Science and Technology, ed. U. Munari (San Francisco, CA: ASP), 237
Szabados, L., Cseh, B., Kovacs, J., et al. 2014, MNRAS, 442, 3155
Szabados, L., Derekas, A., Kiss, C., & Klagyivik, P. 2012, MNRAS, 426, 3154
Templeton, M. R., & Karovska, M. 2009, ApJ, 691, 1470
Tokovinin, A. A. 1987, SvA, 31, 98
Tokovinin, A. 2014, AJ, 147, 87
Wallerstein, G. 1979, PASP, 91, 770
Wolff, S. C. 1978, ApJ, 222, 556